FIGURE 1

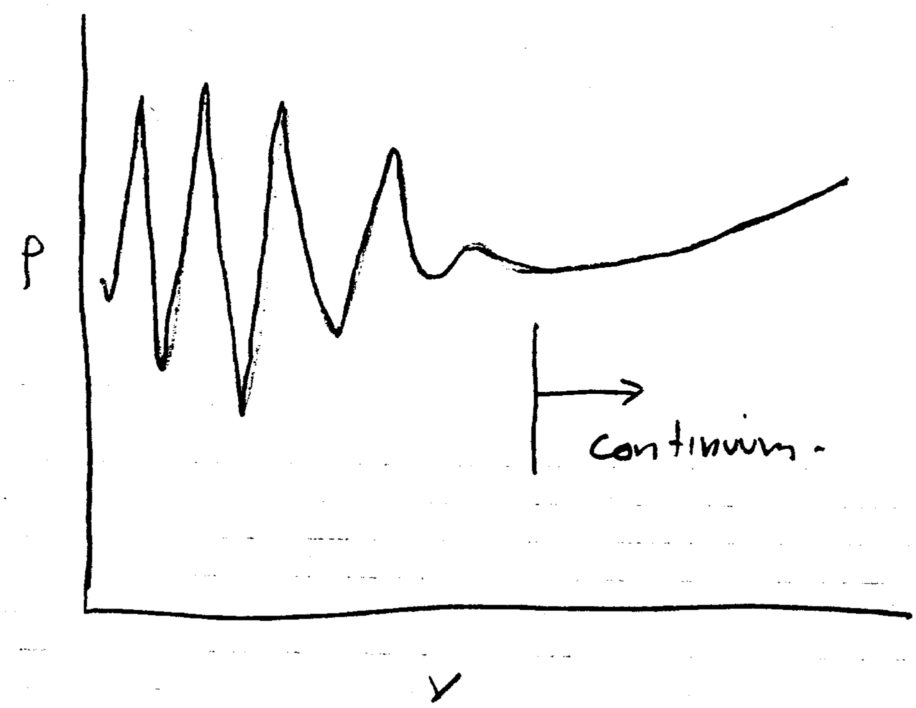

density $\rho \equiv$ mass/volume

FIGURE 2

(a)

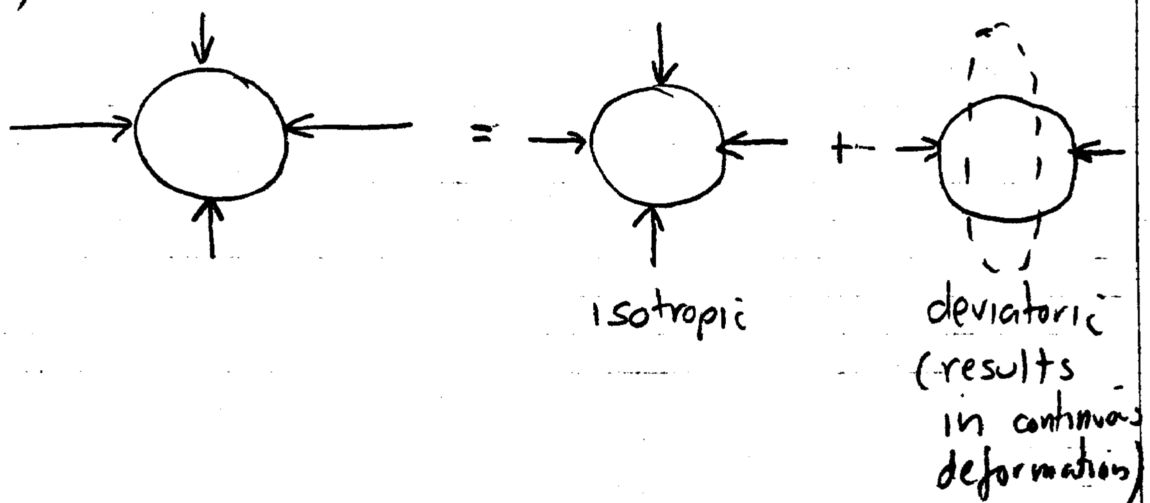

(b)

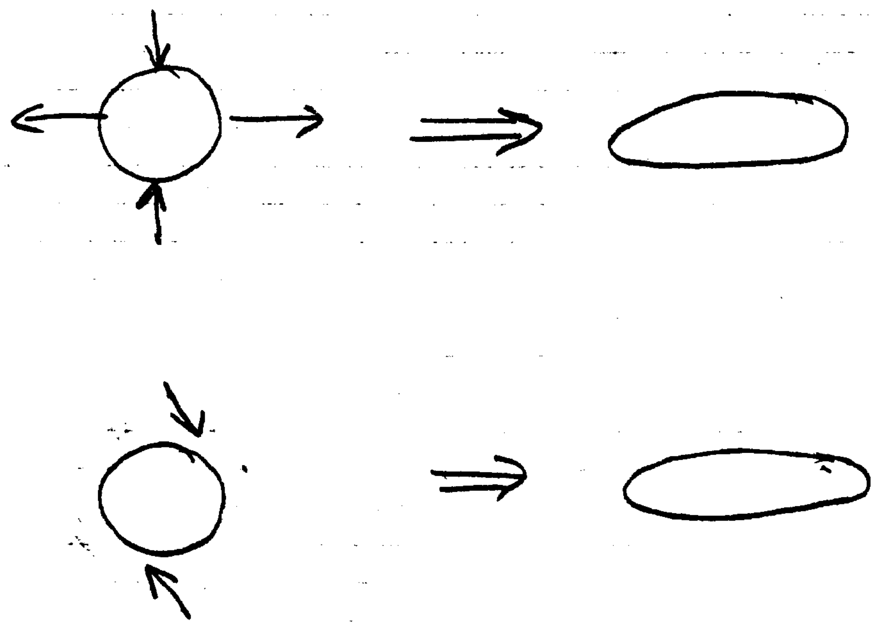

Non-isotropic normal and shear forces are equivalent.

Figure 3.

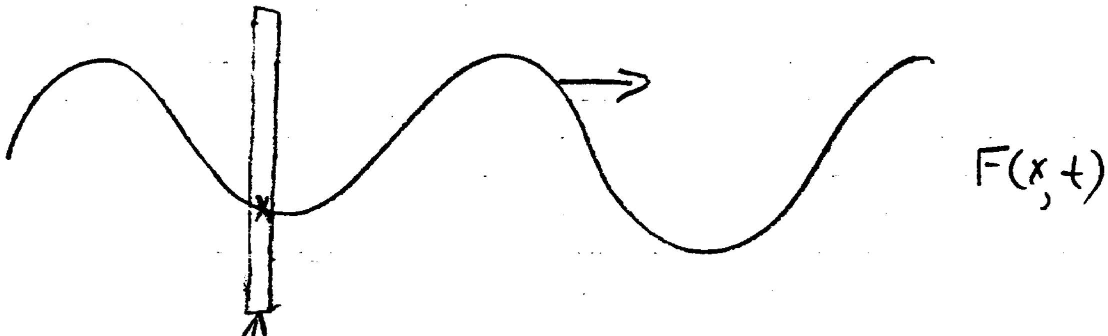

window fixed in space.

F(x,t) is a sinusoid moving to the right:

(a) An observer who moves with F and looks at one point will see a constant.

(b) An observer fixed in space who observers F through a slit which is also fixed will see a value that oscillates up and down.

Figure 4

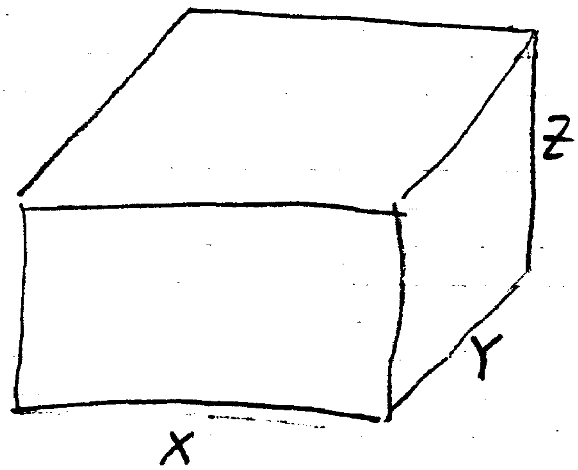

$t = 0$

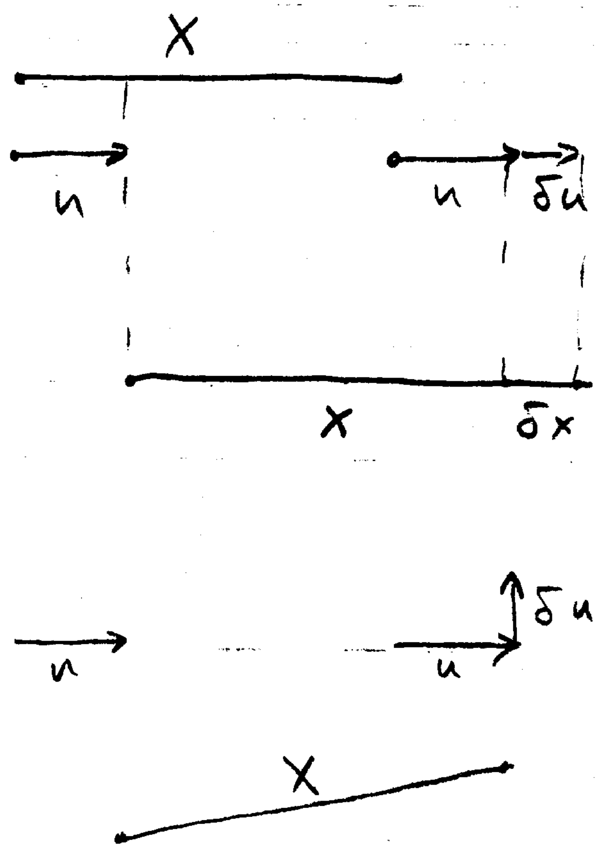

(a) $t = \delta t$

side is <u>stretched</u>

(b) $t = \delta t$

side is <u>rotated</u>.

FIGURE 5

Non-Uniform normal forces acting on a small volume of fluid.

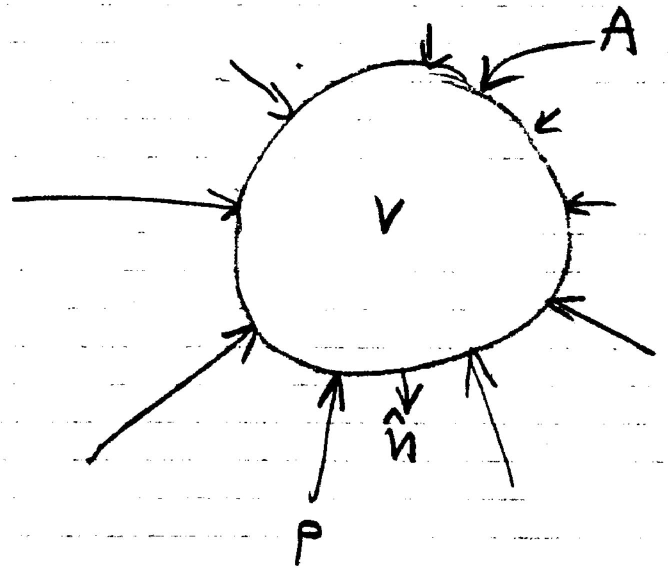

normal force/unit area $= -p\hat{n}$

FIGURE 6

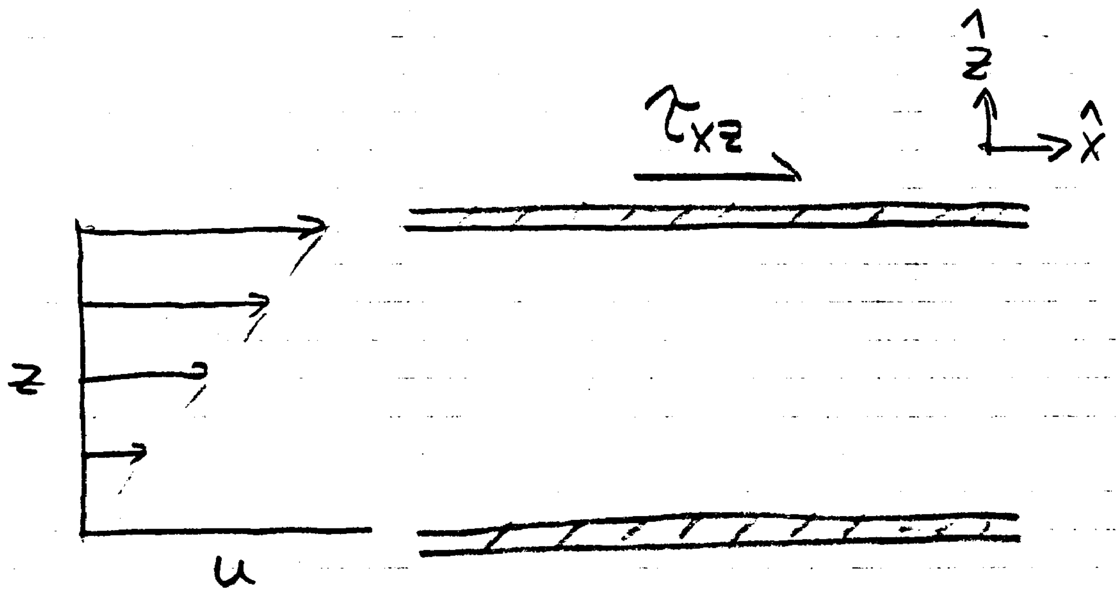

$$\tau_{xz} = \mu \frac{\partial u}{\partial z}$$

Couette Flow

FIGURE 7

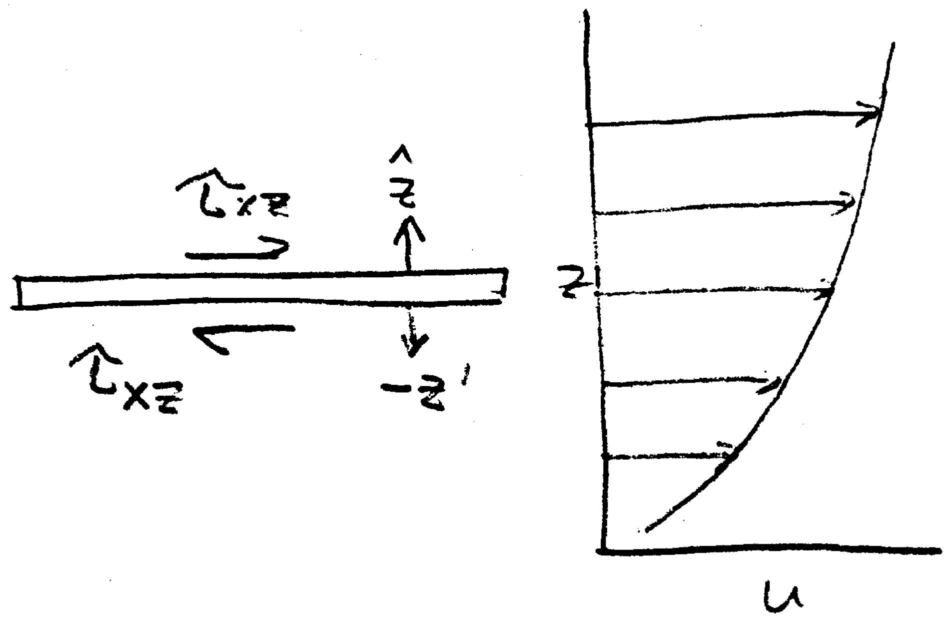

FIGURE 8

(a)

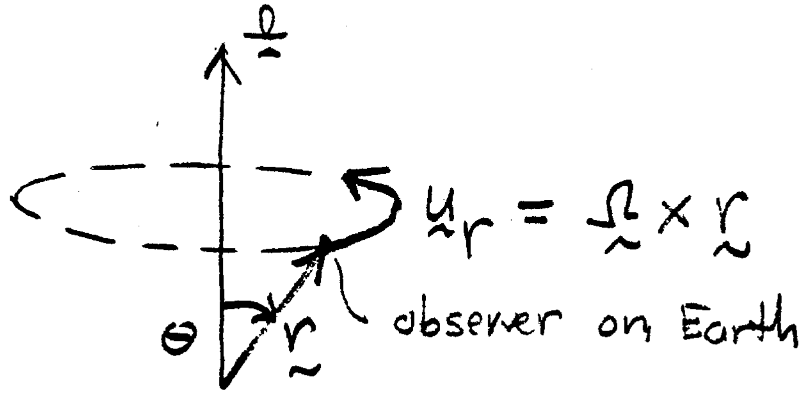

$\underset{\sim}{\Omega}$
$\underset{\sim}{u}_r = \underset{\sim}{\Omega} \times \underset{\sim}{r}$
observer on Earth
θ
$\underset{\sim}{r}$

(b)

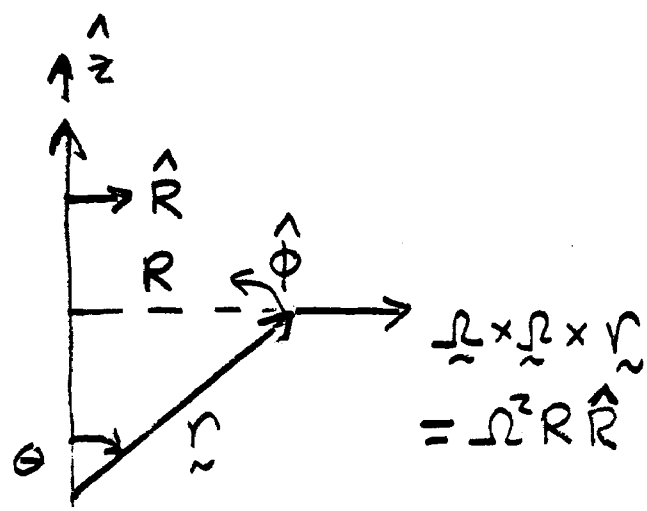

$\hat{z}$
$\hat{R}$
$\hat{\phi}$
R
$\underset{\sim}{\Omega} \times \underset{\sim}{\Omega} \times \underset{\sim}{r}$
$= \Omega^2 R \hat{R}$
θ
$\underset{\sim}{r}$

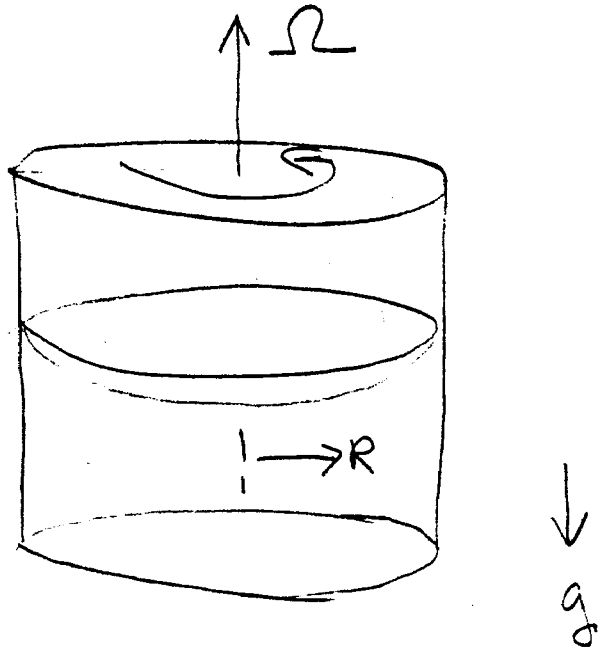

FIGURE 9

FIGURE 10

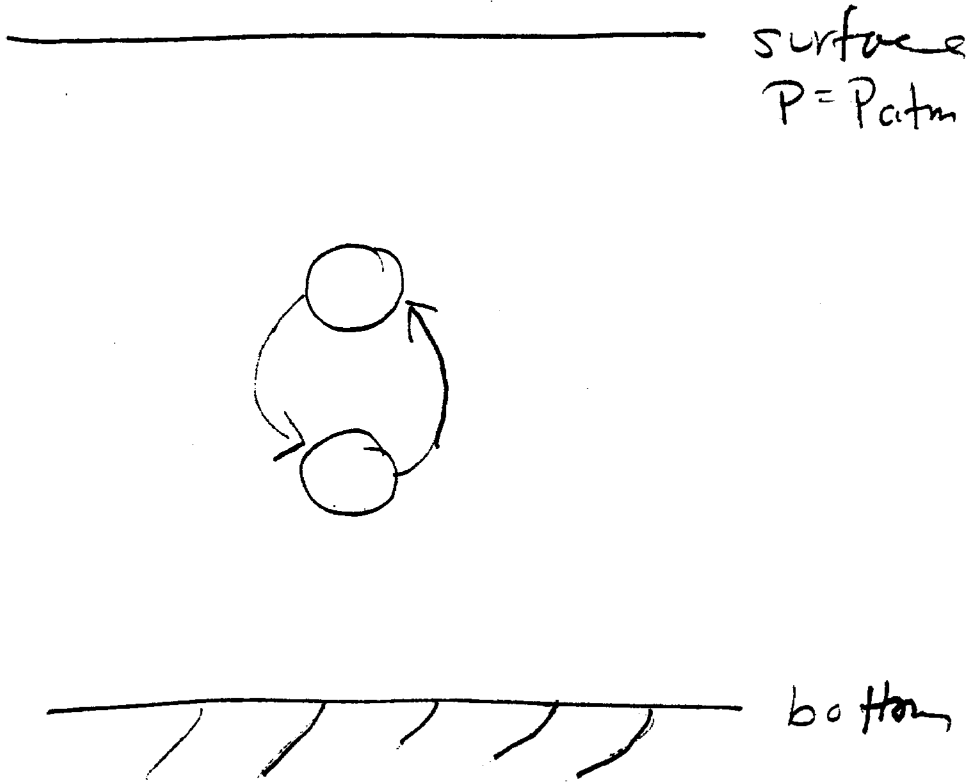

FIGURE 11

(a) Rotating "Couette" Flow (Top View)

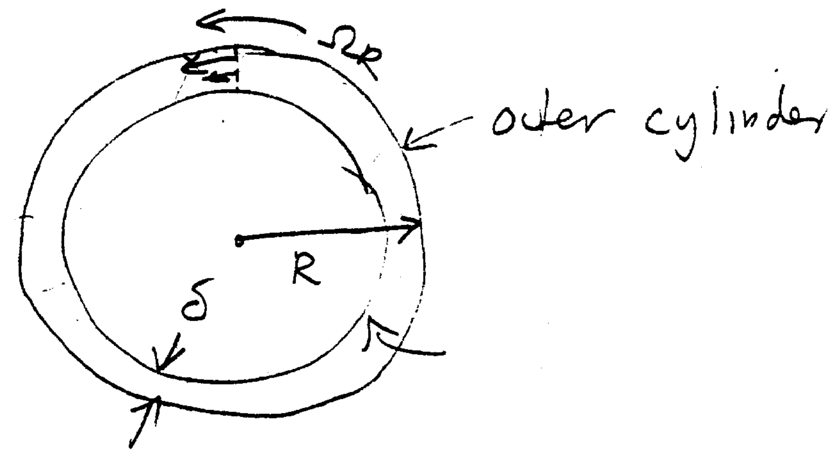

(b) Cone-Plate "Couette" Flow (side view)

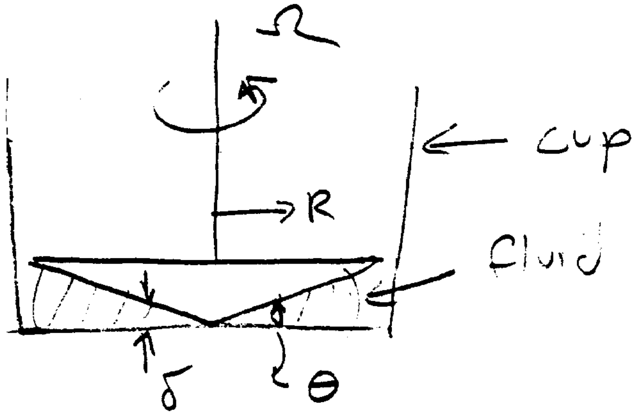

$$u(R) = \Omega R$$
$$\delta(R) = R\tan\theta \simeq R\theta$$
$$\frac{\partial u}{\partial z} = \frac{u}{\delta} = \frac{\Omega}{\theta} = \text{constant}.$$

FIGURE 12

(a) Plane Poiseuille Flow

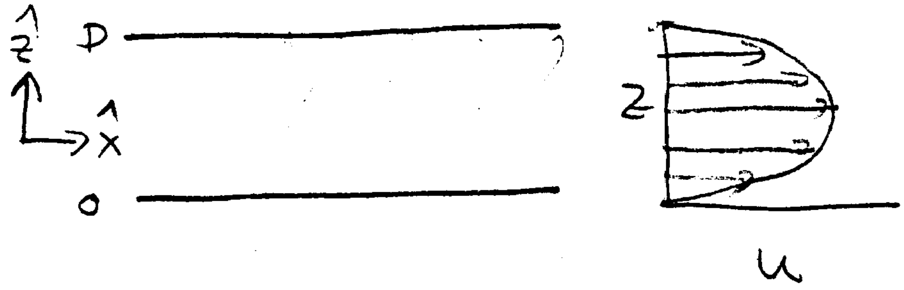

(b) Cylindrical Poiseuille Flow
(Pipe Flow)

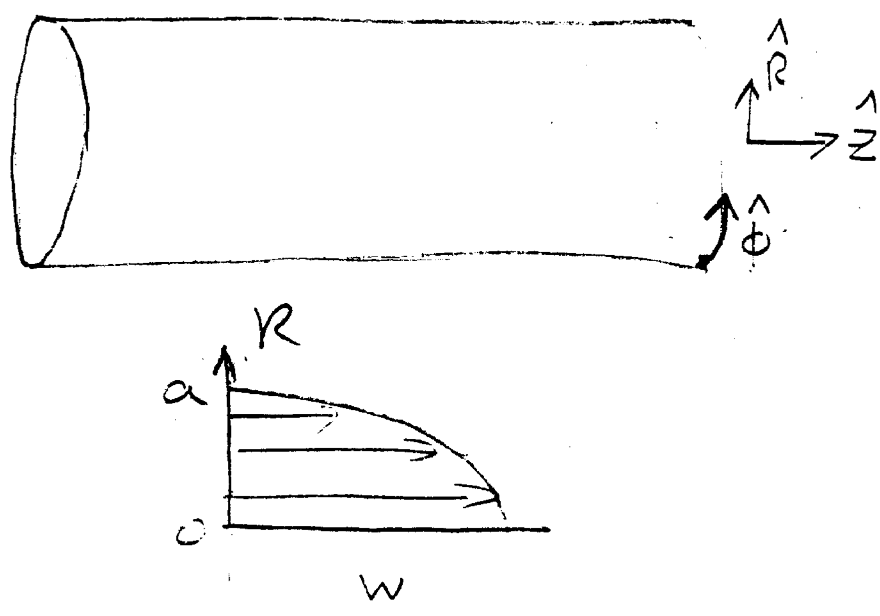

FIGURE 13

(a) Porous medium

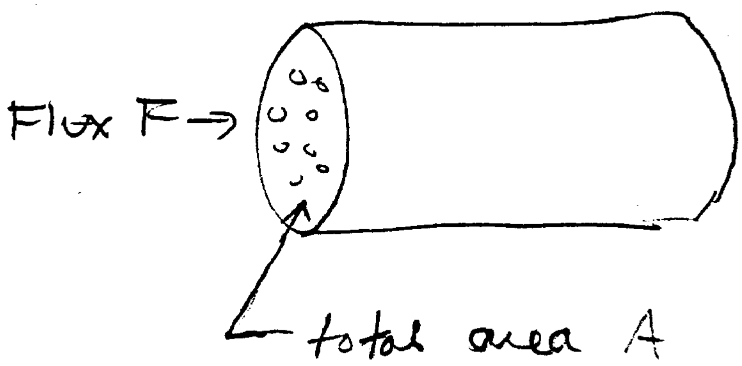

$$u_{avg} = F/A$$

(b) Hele-Shaw Cell

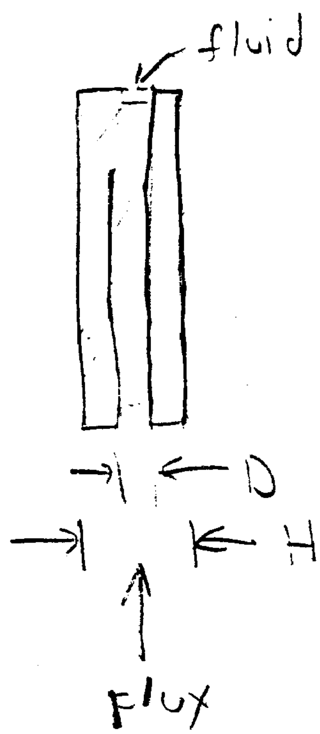

FIGURE 14

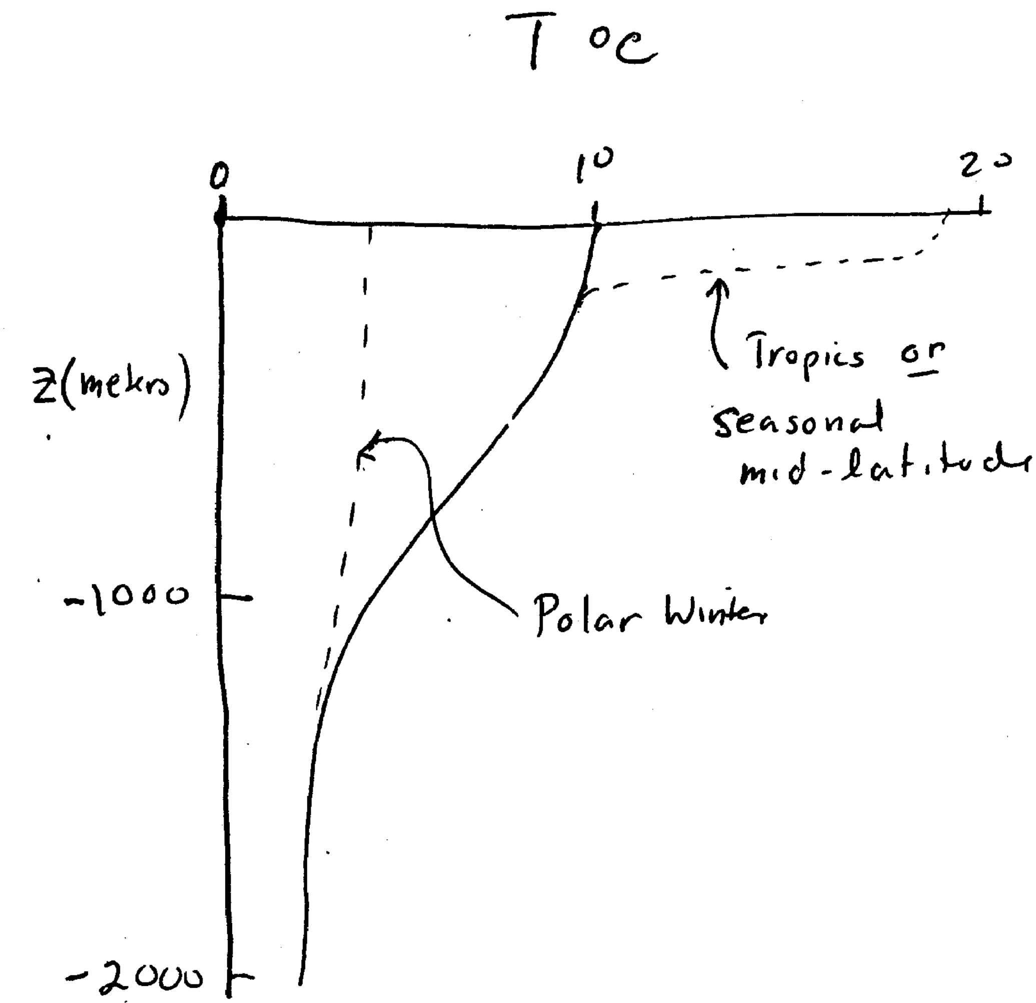

T °C
0
10
20
Z(meters)
-1000
-2000
Tropics or
seasonal
mid-latitude
Polar Winter

FIGURE 15

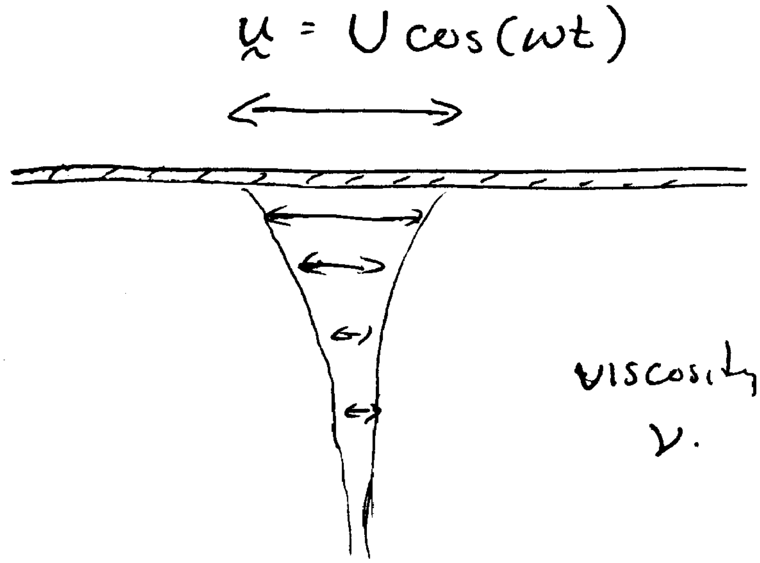

FIGURE 16

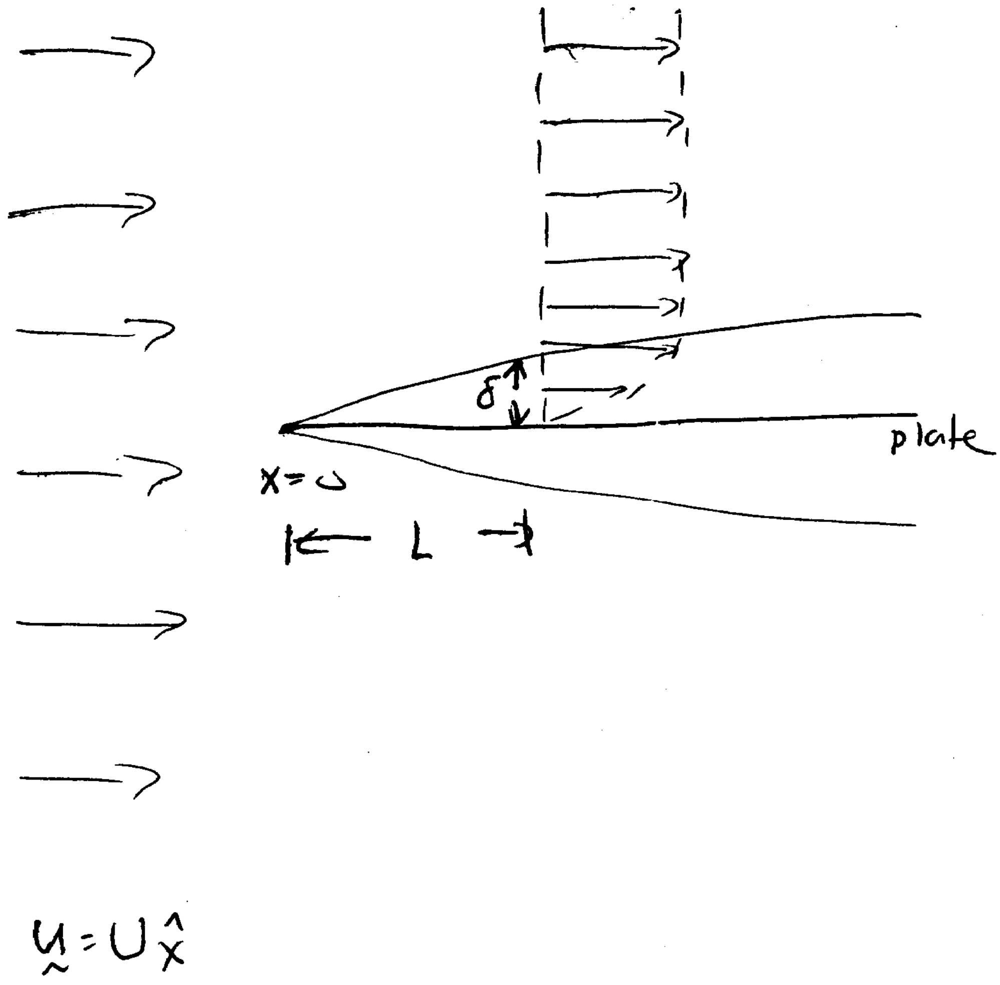

FIGURE 17

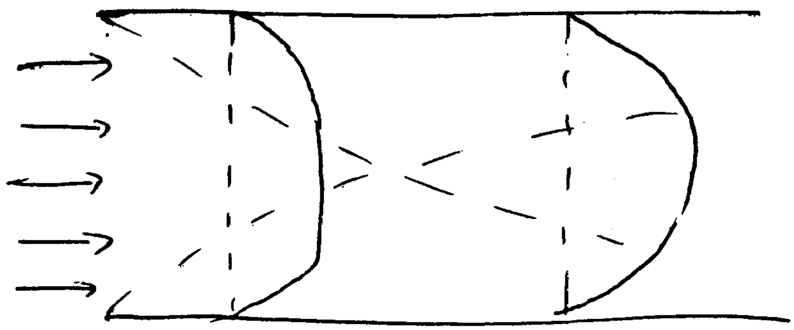

also see figure 2.5 in Tritton

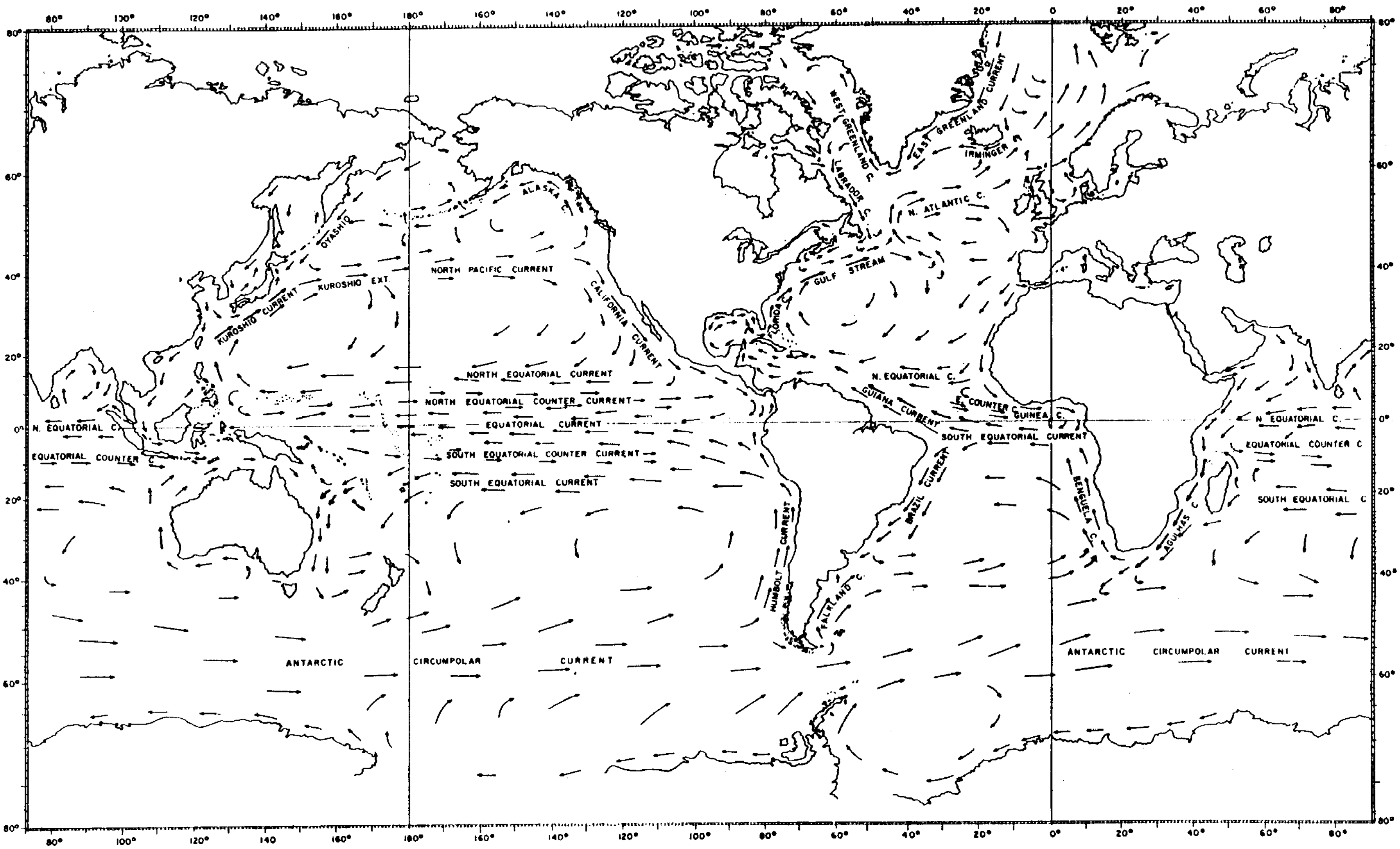
OYASHIO
KUROSHIO EXT
KUROSHIO CURRENT
ALASKA C.
NORTH PACIFIC CURRENT
CALIFORNIA CURRENT
NORTH EQUATORIAL CURRENT
NORTH EQUATORIAL COUNTER CURRENT
EQUATORIAL CURRENT
SOUTH EQUATORIAL COUNTER CURRENT
SOUTH EQUATORIAL CURRENT
N. EQUATORIAL C.
EQUATORIAL COUNTER C.
WEST GREENLAND C.
EAST GREENLAND CURRENT
IRMINGER
LABRADOR C.
N. ATLANTIC C.
GULF STREAM
FLORIDA
N. EQUATORIAL C.
GUIANA CURRENT
E. COUNTER C.
GUINEA C.
SOUTH EQUATORIAL CURRENT
BRAZIL CURRENT
HUMBOLT CURRENT
FALKLAND C.
BENGUELA C.
AGULHAS C.
N. EQUATORIAL C.
EQUATORIAL COUNTER C
SOUTH EQUATORIAL C
ANTARCTIC
CIRCUMPOLAR
CURRENT
ANTARCTIC CIRCUMPOLAR CURRENT

FIGURE 18

FIGURE 19

(a)

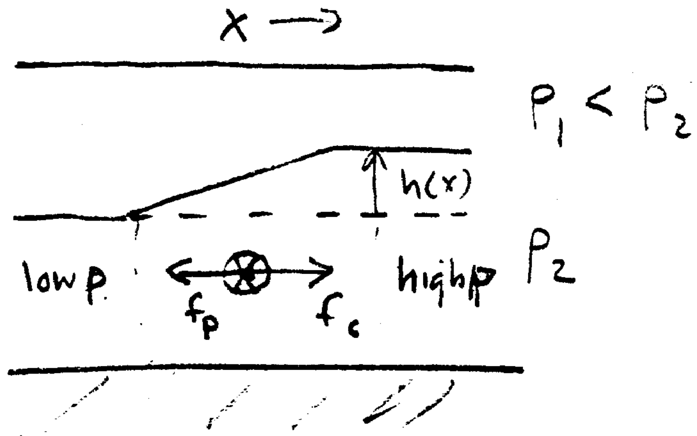

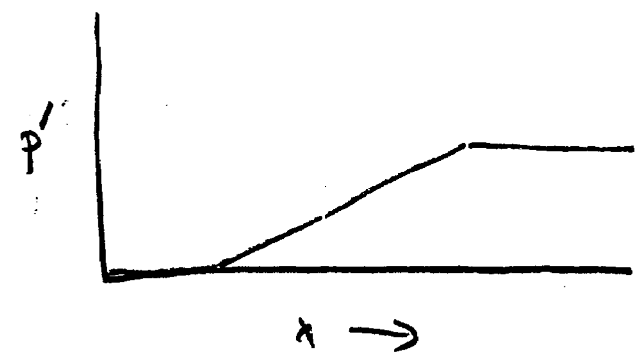

p' = deviation from hydrostatic pressure.

There is a baroclinic geostrophic current northward (in N. hemi.) in lower layer.

(b)

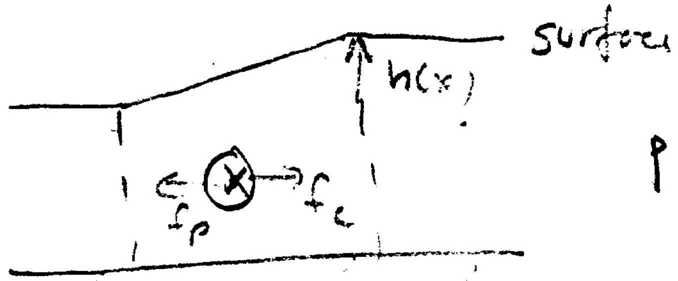

$p' = \rho g\, h(x)$

The pressure gradient force $\nabla p'$ is independent of depth. There is a barotropic geostrophic current at all depths.

FIGURE 20

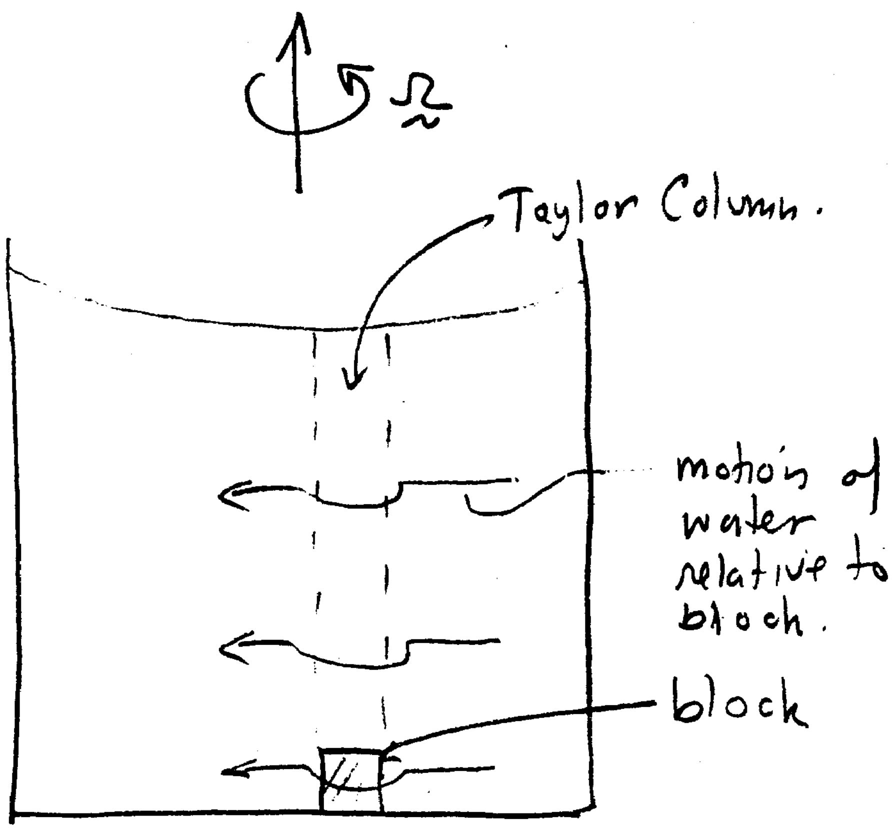

Block moves very slowly relative to rotating tank.

FIGURE 21

(a)

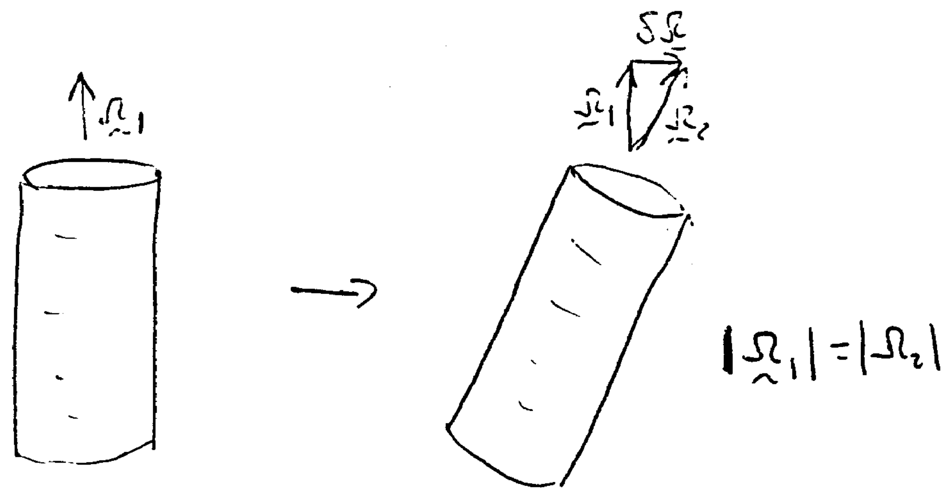

Twisting (or tilting)

(b)

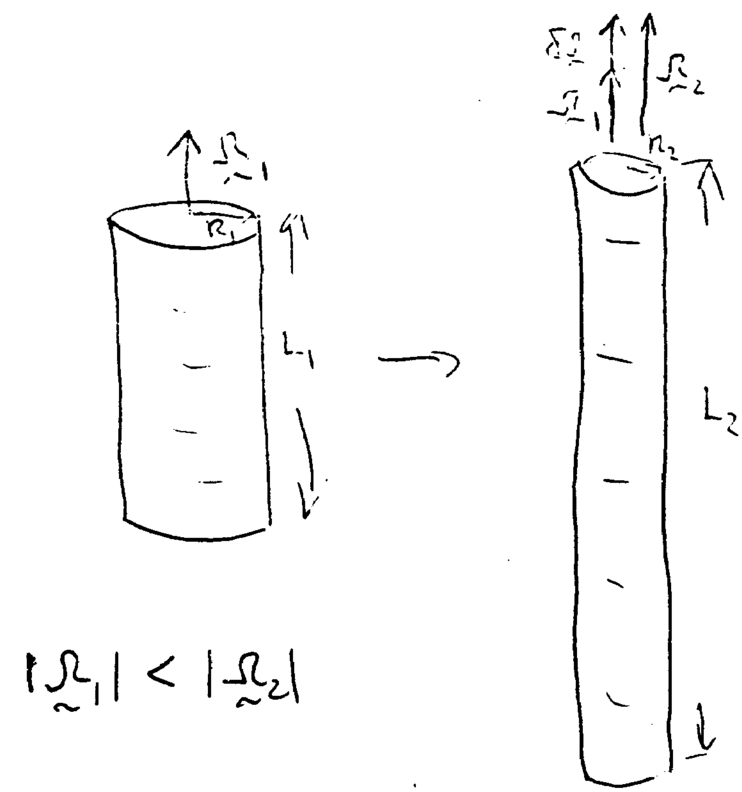

stretching

FIGURE 22

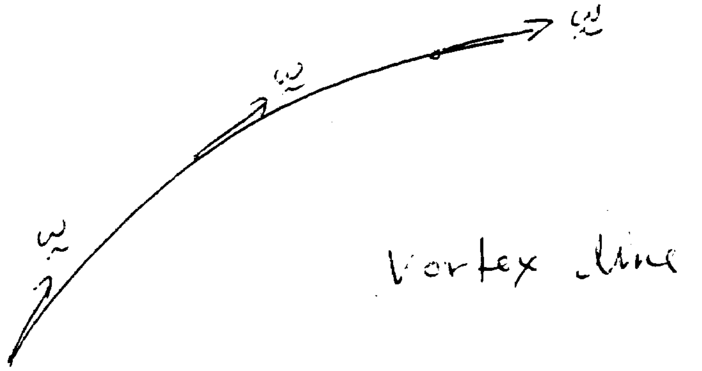

$\omega \cdot \nabla u$

$u \parallel \omega$

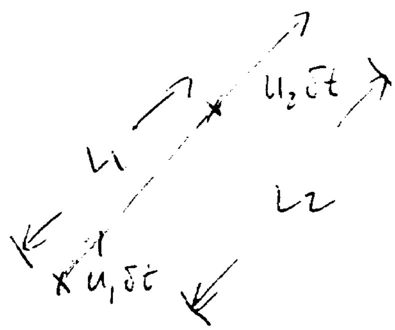

$u_2 > u_1 \Rightarrow L_2 > L_1$

$u \perp \omega$

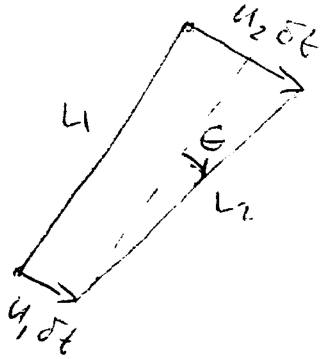

$u_2 > u_1 \Rightarrow \theta > 0$

δt small, $L_1 \simeq L_2$

FIGURE 23

Bernoulli's Theorem $\Rightarrow$ p inversely proportional to $|\underset{\sim}{u}|^2$.

(a) Airfoil

velocity above airfoil higher due to <u>longer path</u>.

(b) Venturi

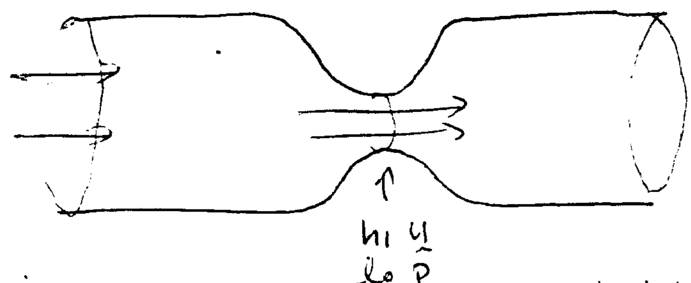

velocity in constriction is high due to small cross section.

(c) Corrugation

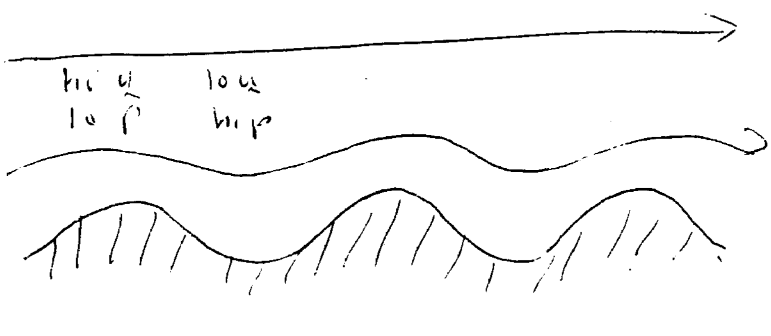

FIGURE 24

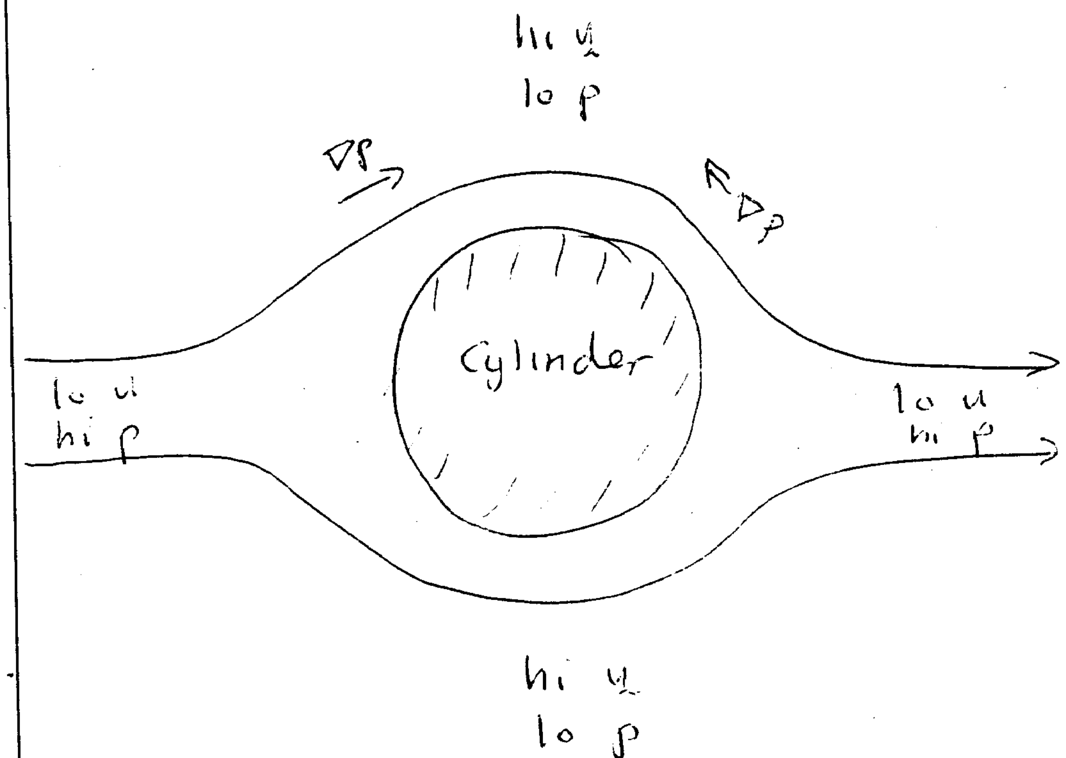

Note that ∇p is in direction needed to accelerate fluid.

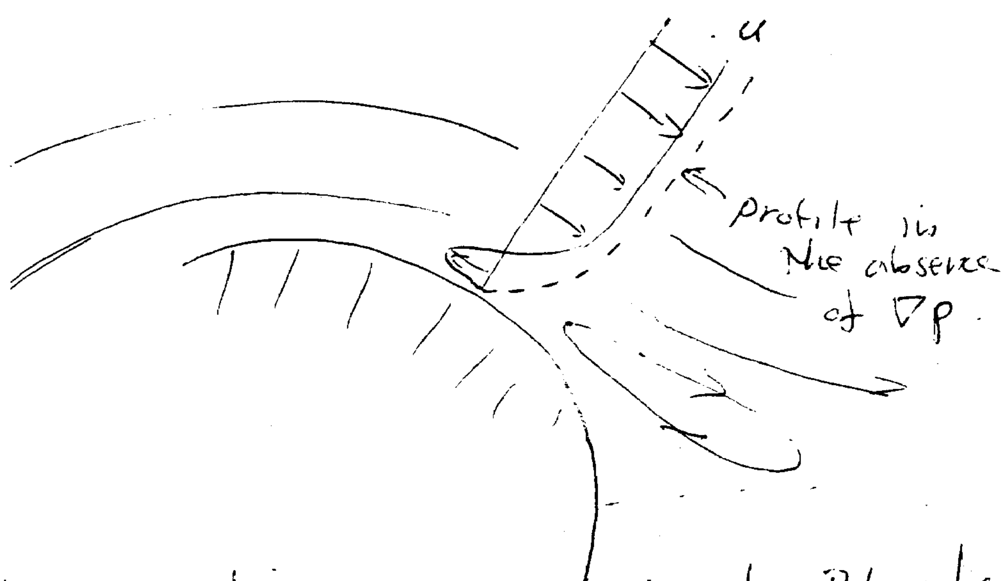

Flow separation can occur in the B.L. when ∇p reverses local flow.

FIGURE 25

f_c = centrifugal force due to rotation (decreases in boundary layer)

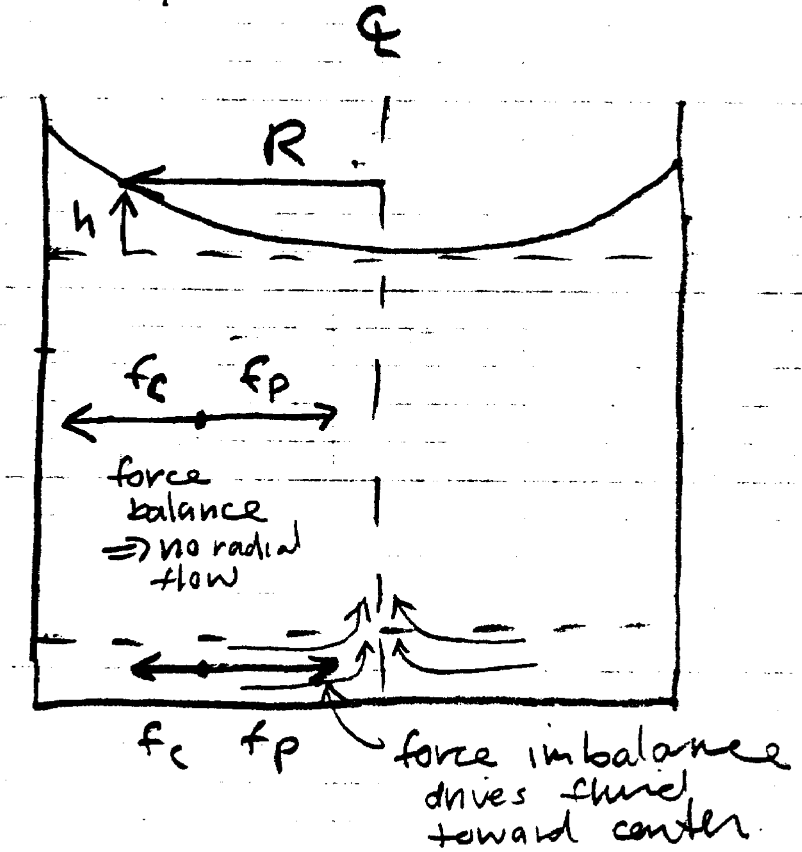

f_p = pressure gradient force due to tilt of surface (increases linearly with R ⇒ slope increases with R).

FIGURE 26

(a) Ekman Spiral (side view)

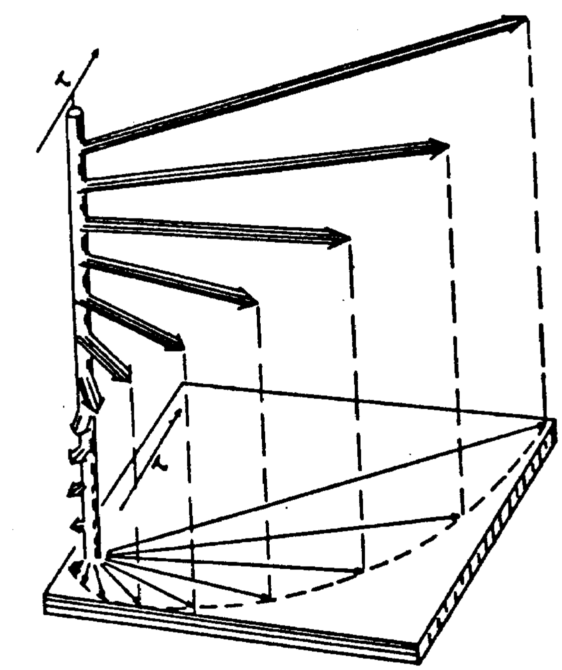

(b) Ekman layer on top of stationary fluid

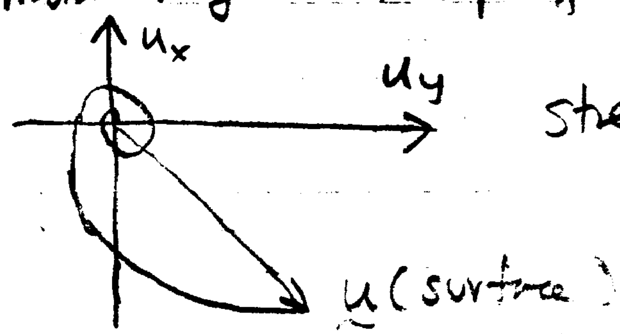

(c) Ekman layer on fixed lower boundary

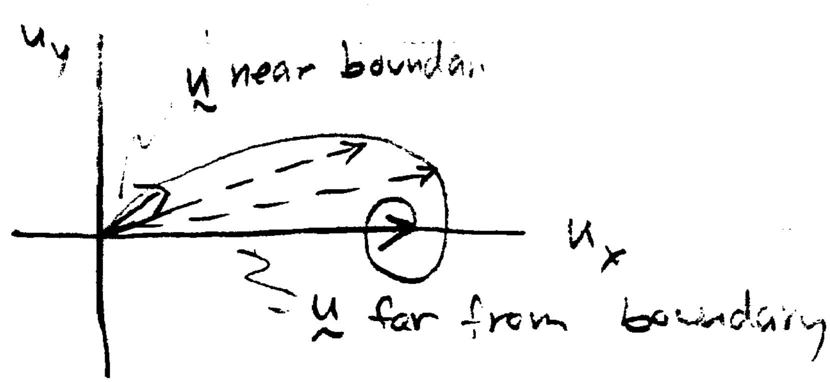

FIGURE 27

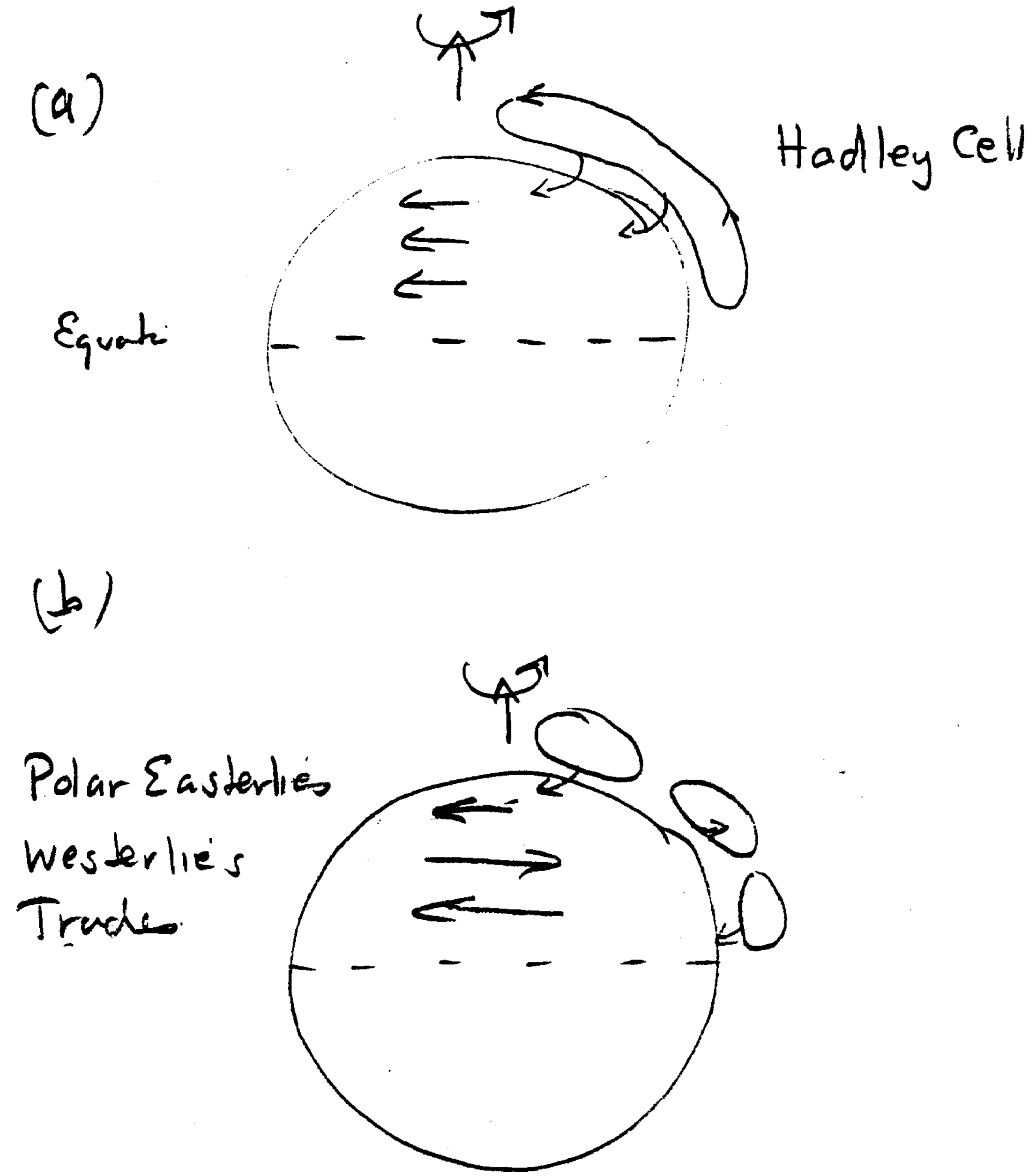

(a)
Hadley Cell
Equator
(b)
Polar Easterlies
Westerlie's
Trades

FIGURE 28

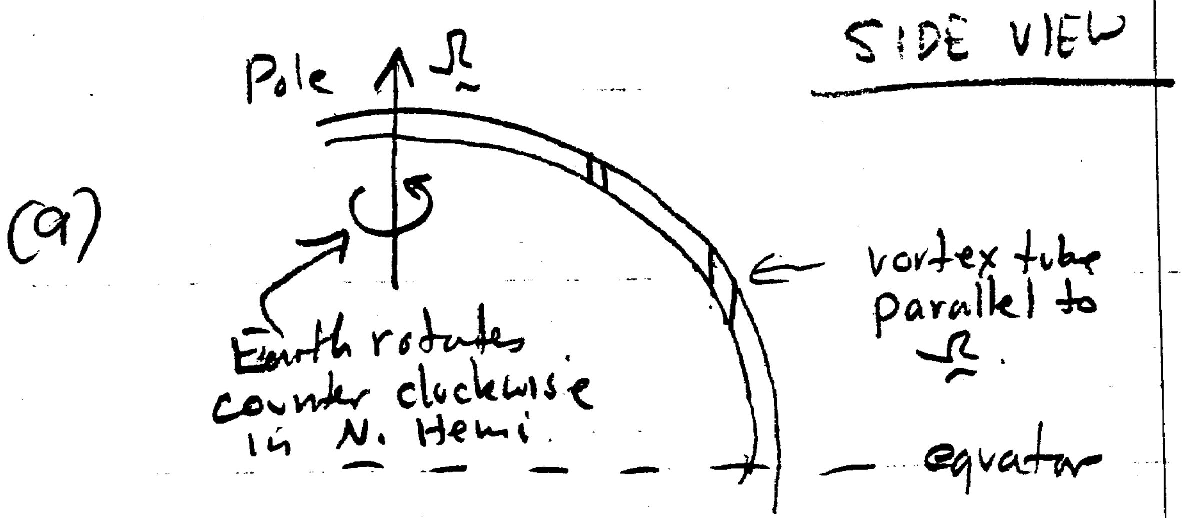

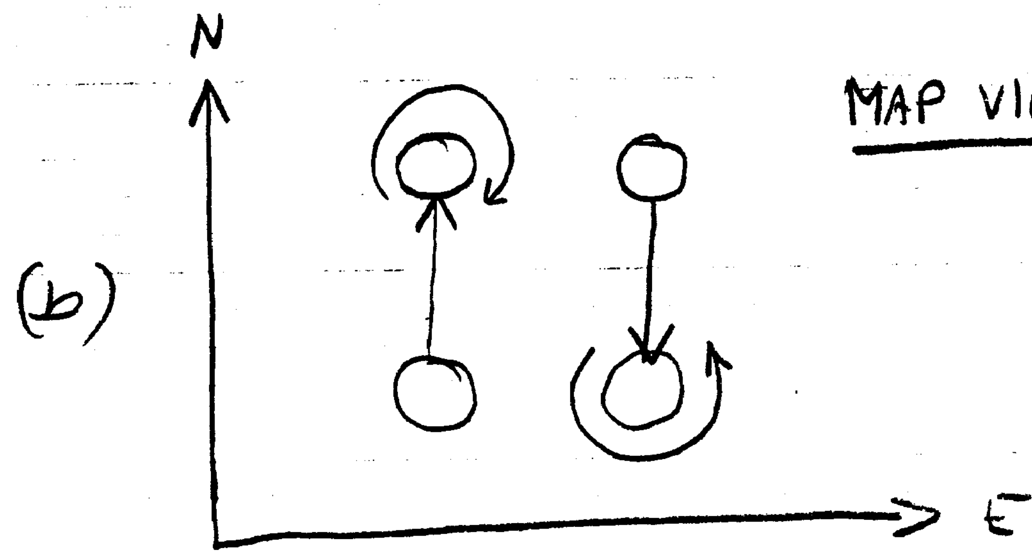

Northward displacement creates clockwise rotation [shortens vortex tube]

Southward displacement creates counter clockwise rotation [stretches vortex tube]

FIGURE 29

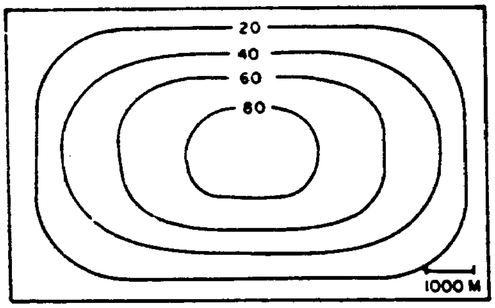

A. NON ROTATING OR UNIFORMLY ROTATING OCEAN
(STOMMEL 1948 FIG. 2)

No stetching of vortex tubes

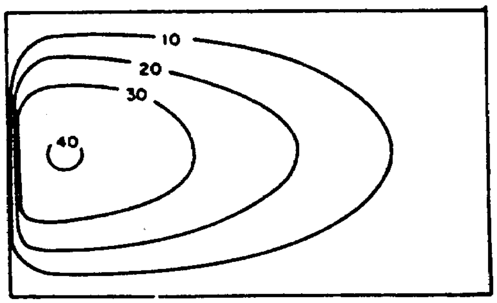

B. CORIOLIS PARAMETER A LINEAR FUNCTION OF LATITUDE (STOMMEL 1948 FIG. 5)

Stetching linearly proportinal to latitude

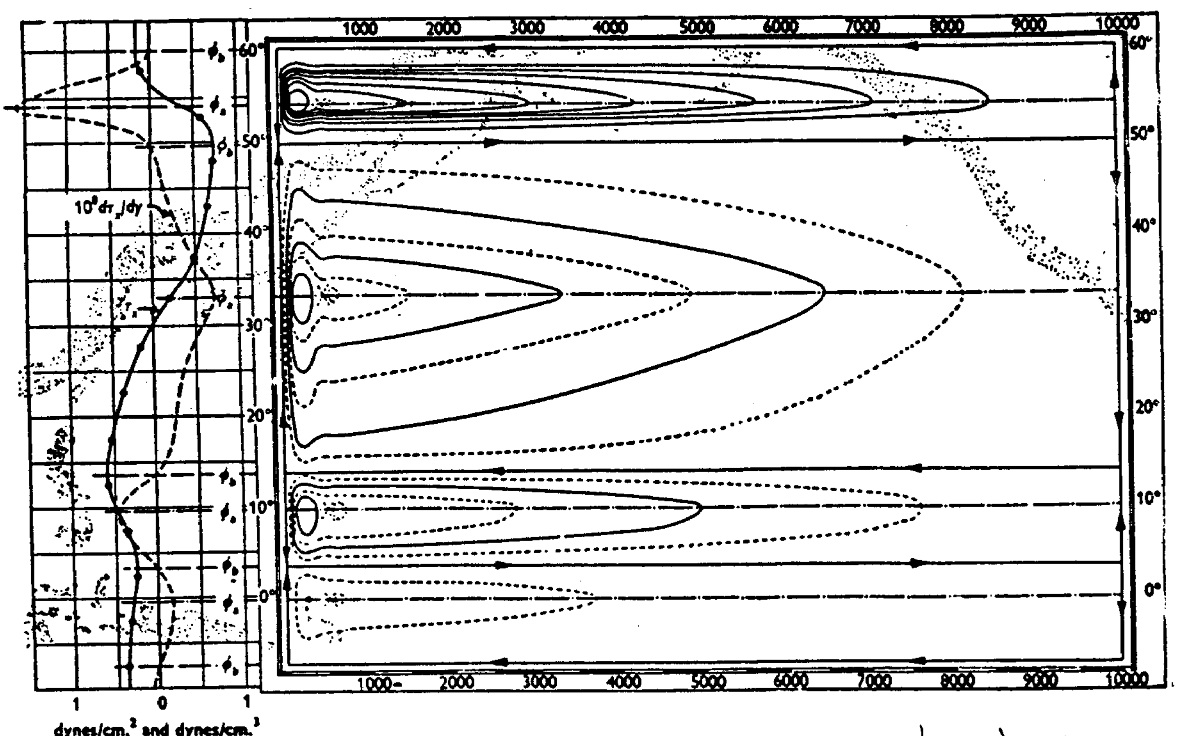

More realistic picture

—— wind

- - - - wind stress

Figure 30(a)

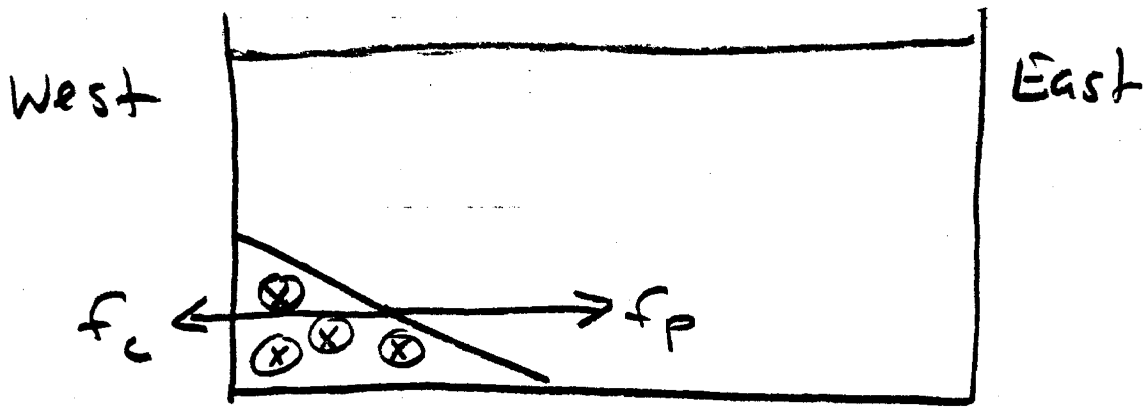

Schematic crosssection of South Atlantic

Fig. 30(b)

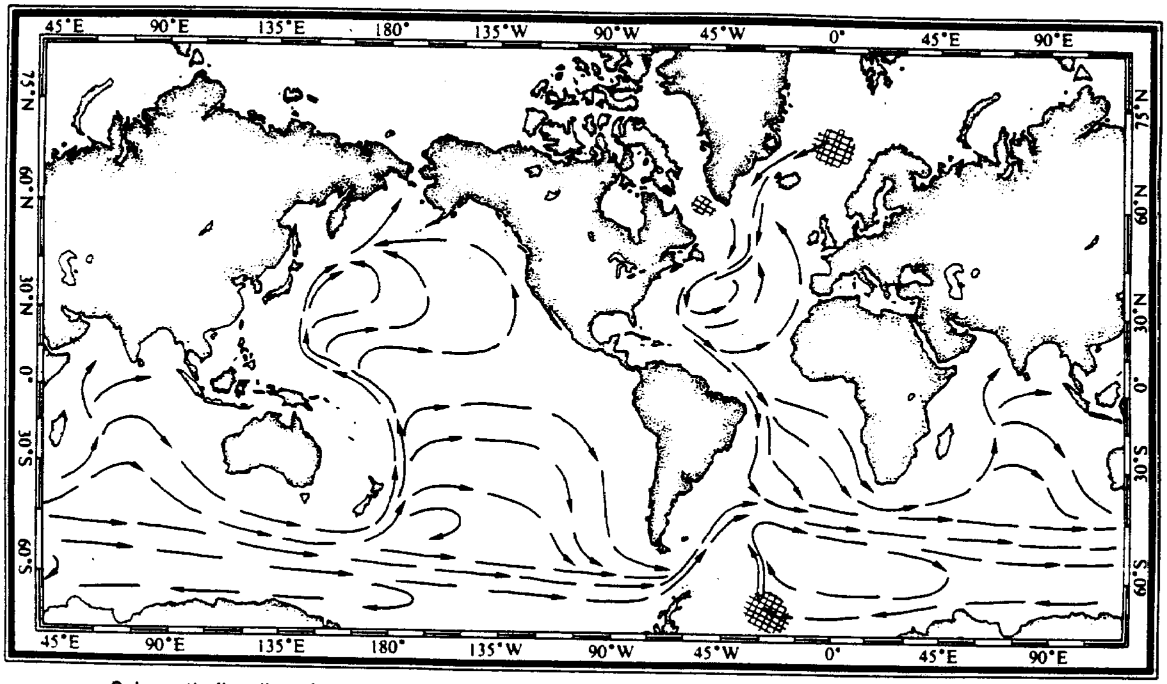

Schematic flow lines for abyssal circulation. The cross-hatched areas indicate regions of production of bottom water. [Adapted from Stommel, H., *Deep Sea Research* (1958).]

Fig. 30(c)

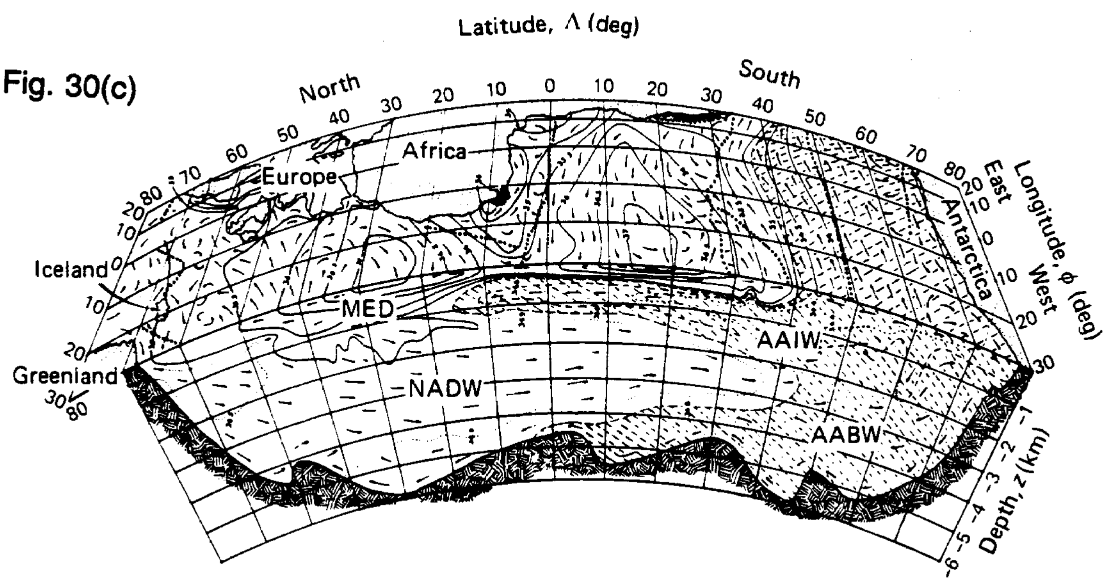

Schematic cross section of surface and subsurface currents in the North and South Atlantic. [Adapted from Wüst, G., *Kieler Meeresforschungen* (1950).]

Figure 31

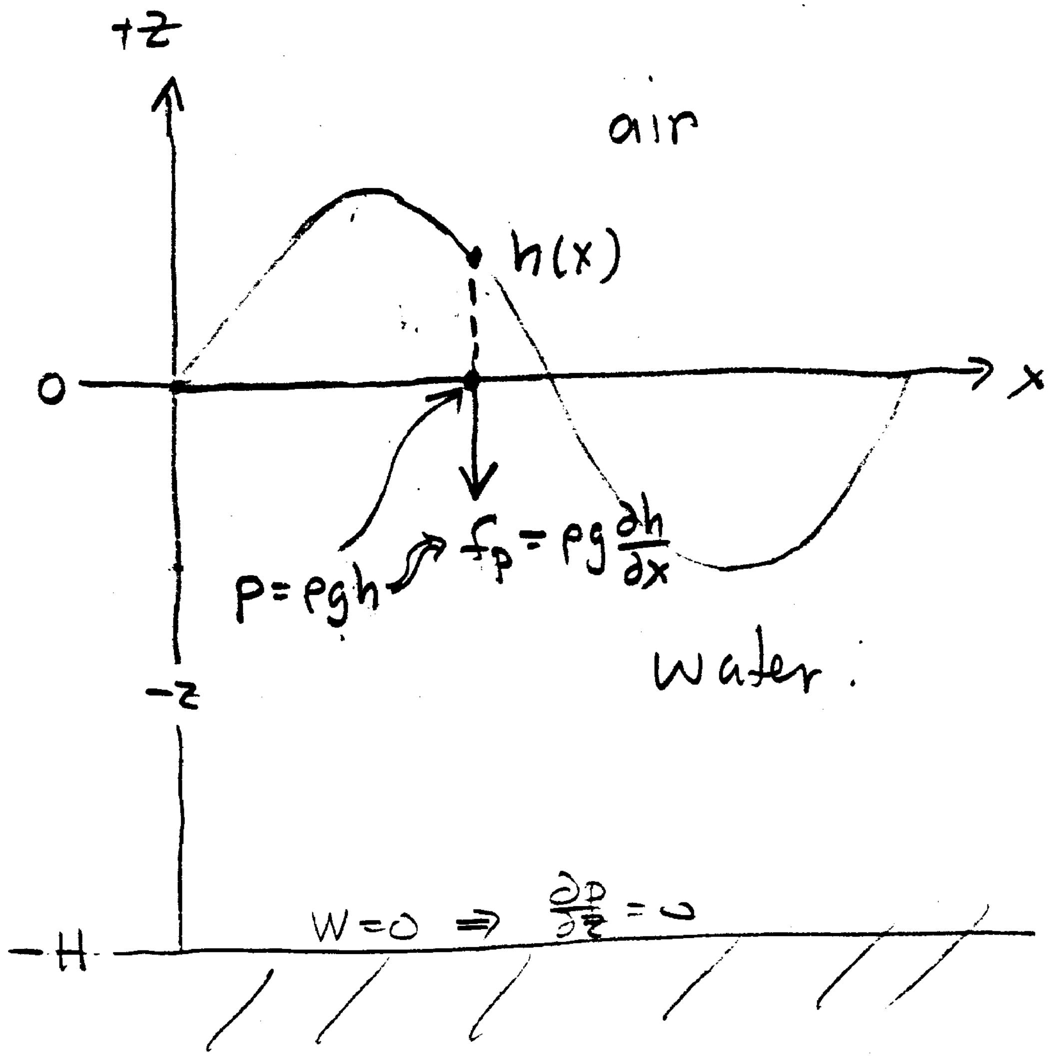

+z
air
h(x)
0
x
$P = \rho g h$
$f_p = \rho g \frac{\partial h}{\partial x}$
water.
-z
$-H$
$W = 0 \Rightarrow \frac{\partial p}{\partial z} = 0$

Figure 32

(a)

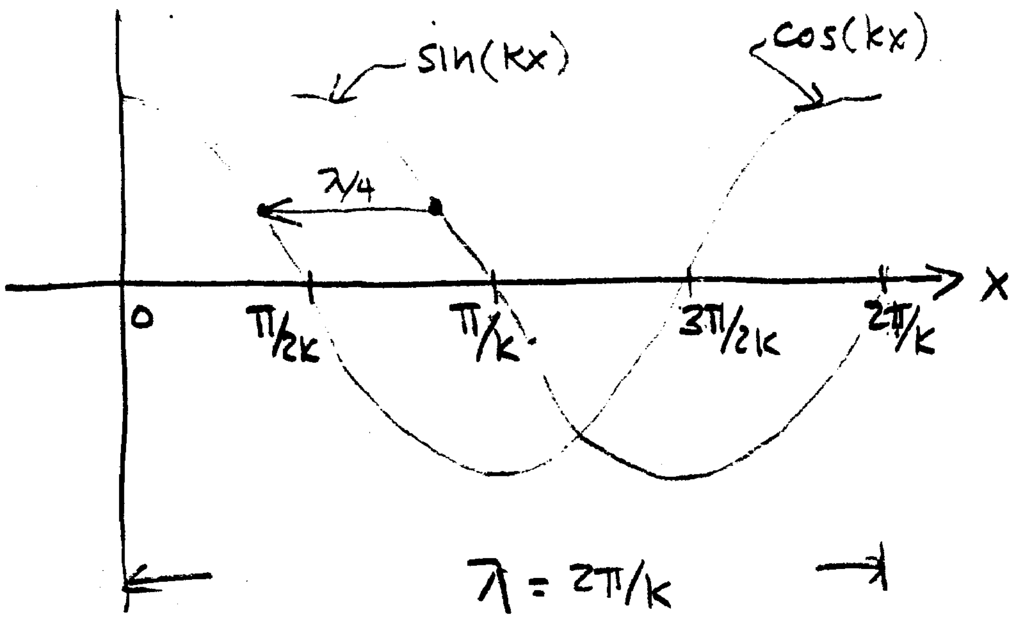

(b)

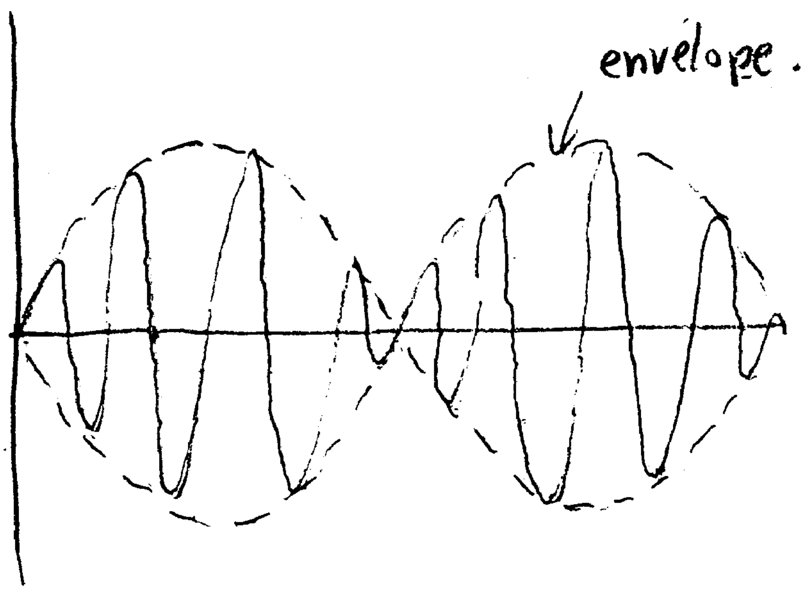

Figure 33

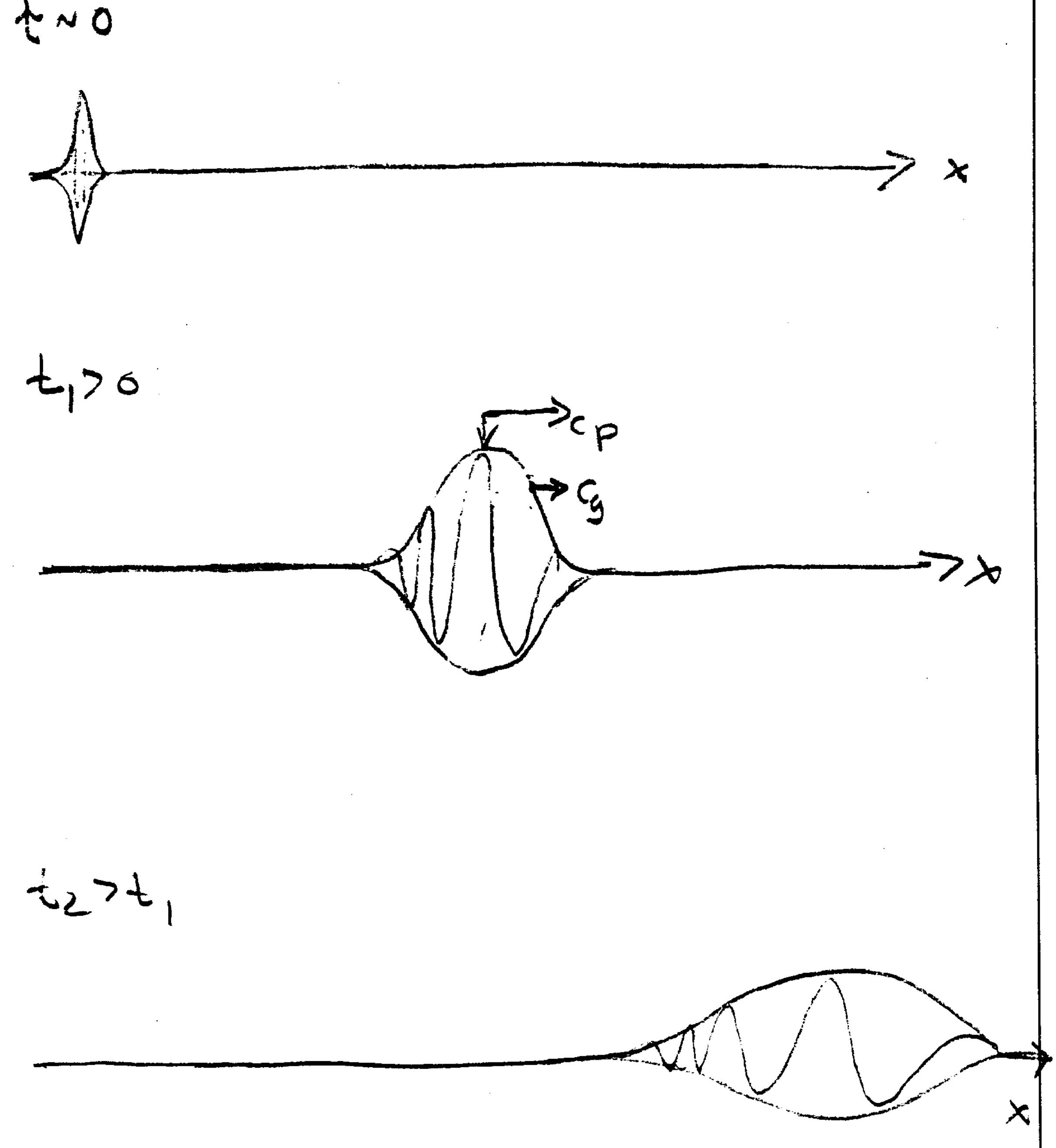

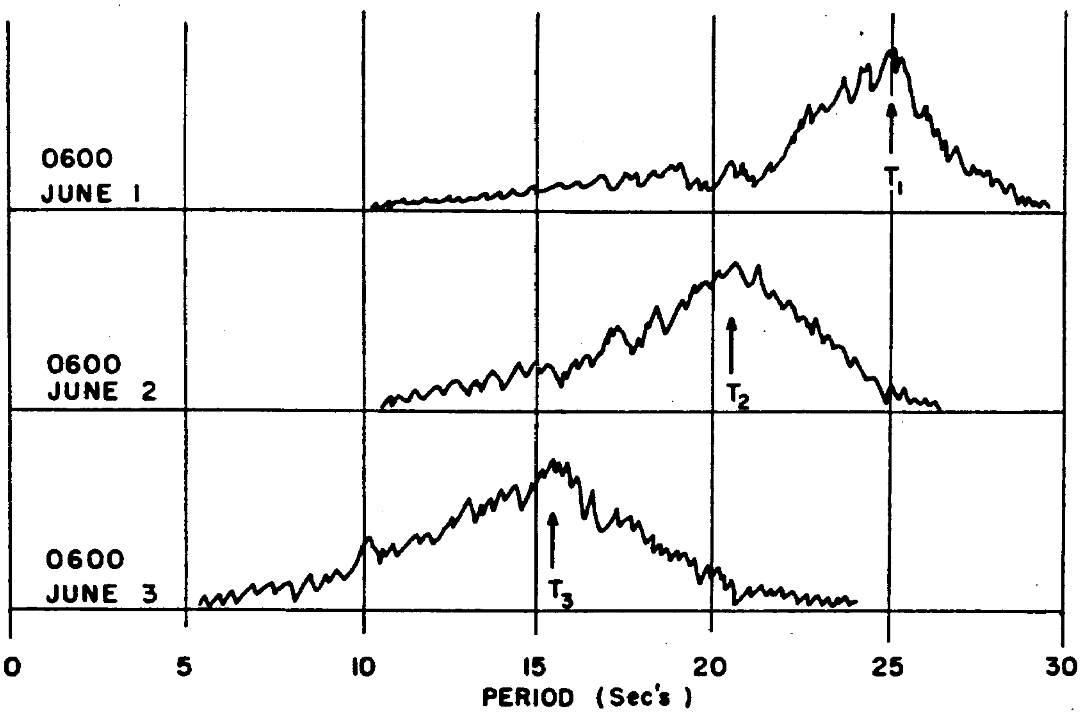

Fig. 34. Wave energy spectra on successive days at a coastal site

FIGURE 35

Fluid motion in surface gravity waves.

(a) Deep water.

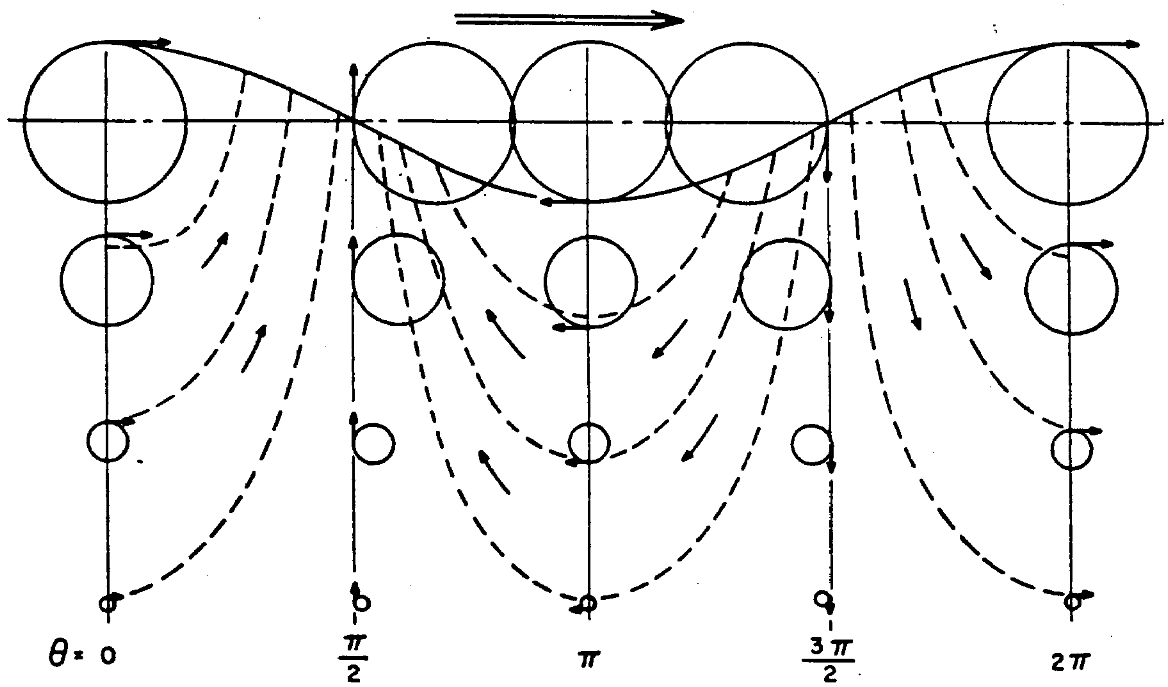

(b) Shallow water

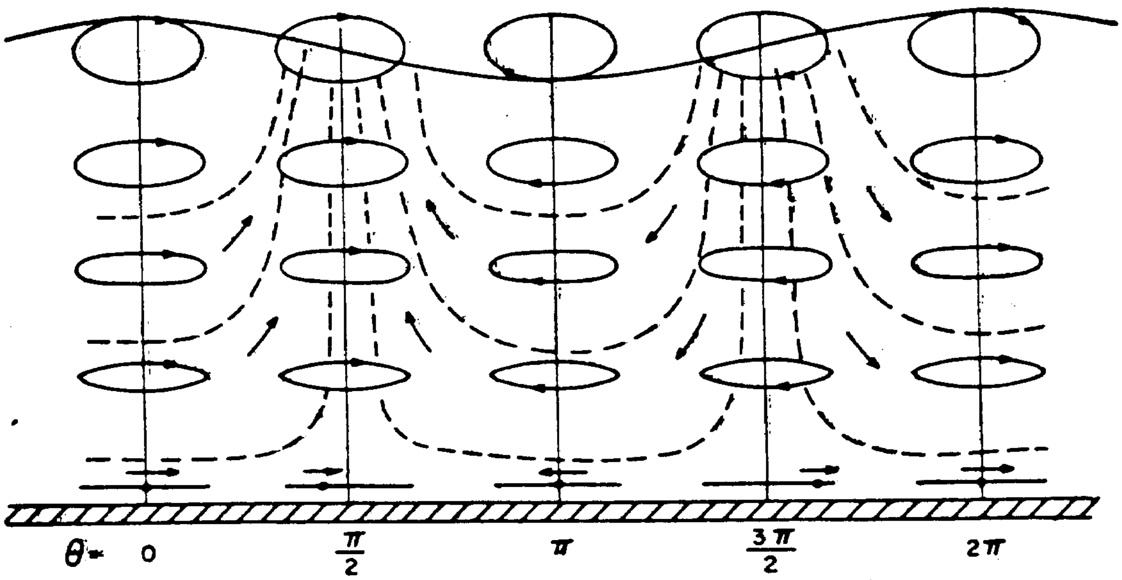

Figure 36 – Deep and shallow water waves; period = 10 s

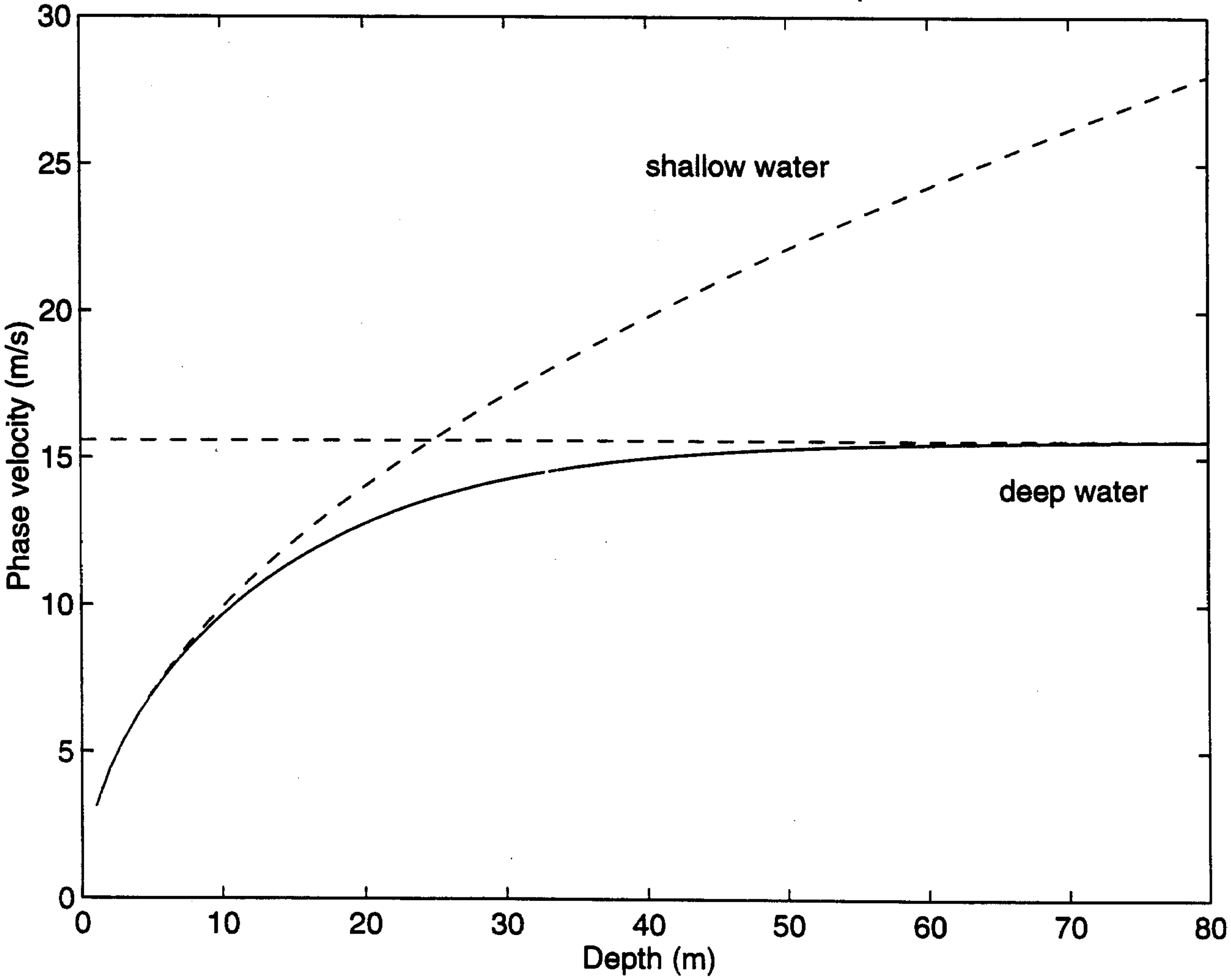

FIGURE 37

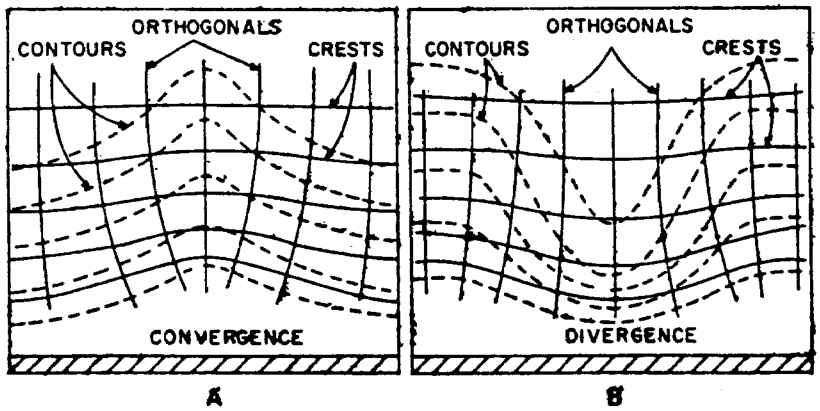

Wave crest convergence (focussing) and divergence (de-focussing) due to bottom contours. Wave energy is focussed on a ridge (which would erode the ridge).

Figure. 38

Linear wave

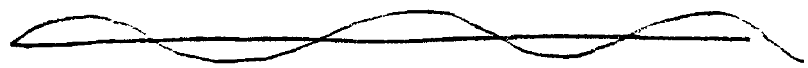

Weakly non-linear wave

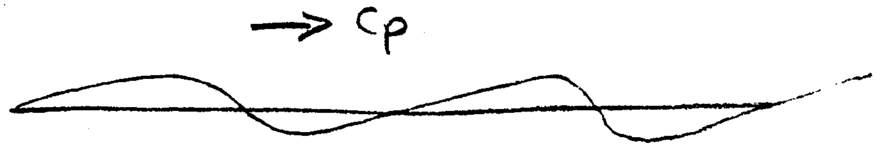

Strongly non-linear wave

Bore (shock wave)

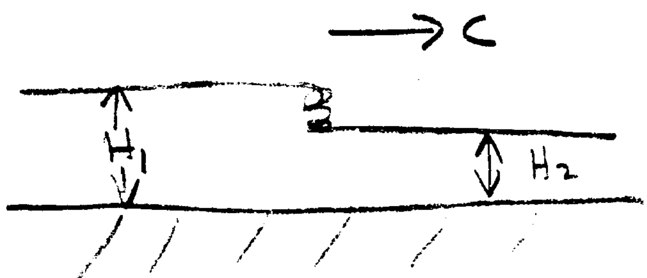

$$\sqrt{gH_1} \geq c > \sqrt{gH_2}$$

FIGURE 39

Kelvin Wave

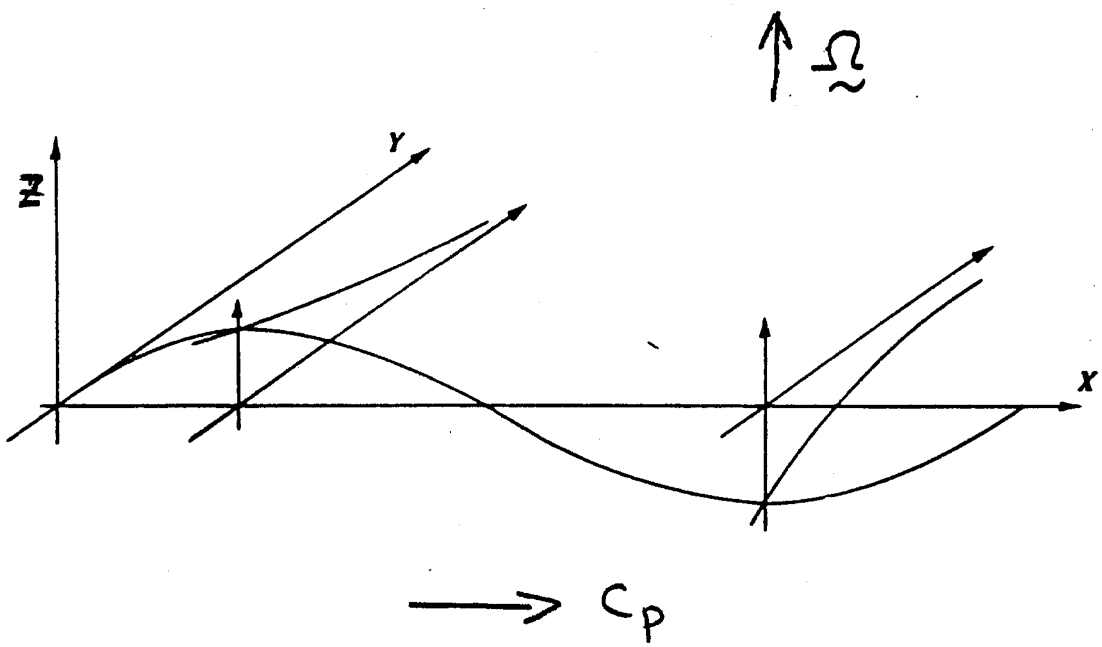

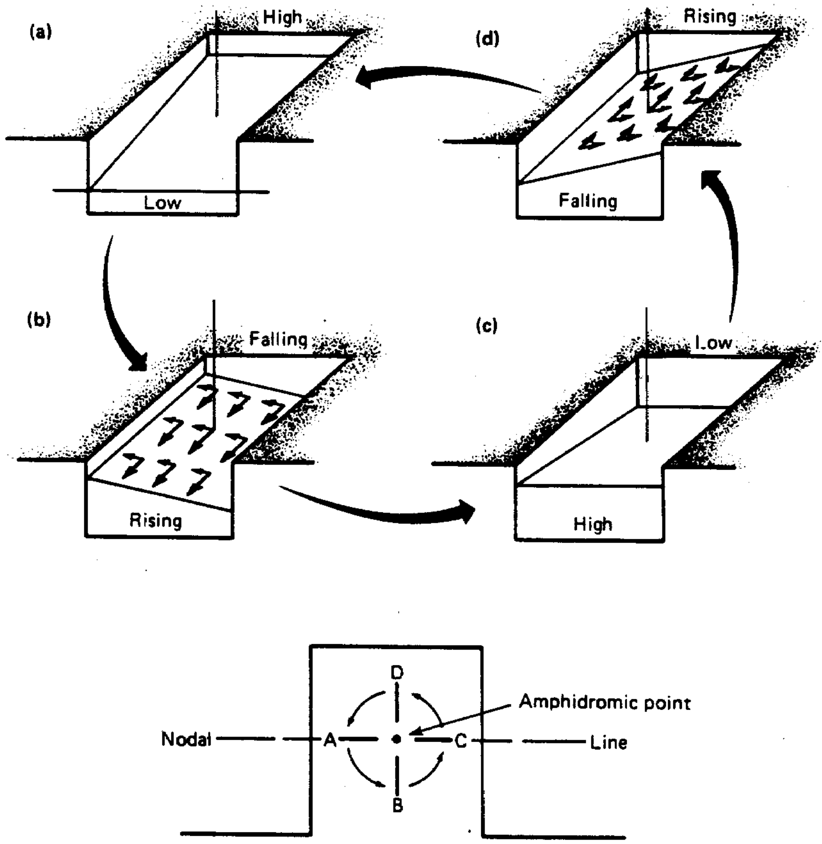

Fig. 40(a) Schematic of rise and fall of tides in an embayment in the Northern Hemisphere. Tidal elevations appear to rotate counterclockwise about the amphidromic point. [Adapted from von Arx, W. S., *An Introduction to Physical Oceanography* (1962).]

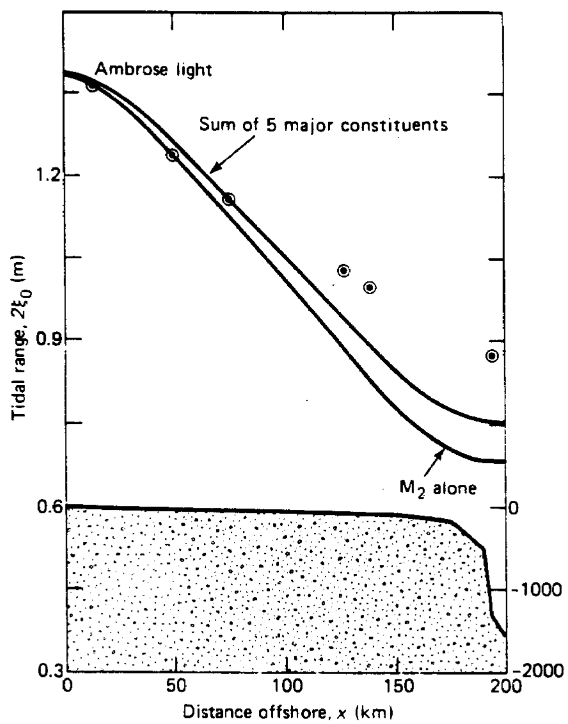

Fig. 40(b) Transition of tidal amplitude from New York harbor across the continental shelf to the shelf break. [Adapted from Schwiderski, E. W., *Rev. Geophys. and Space Phys.* (1980).]

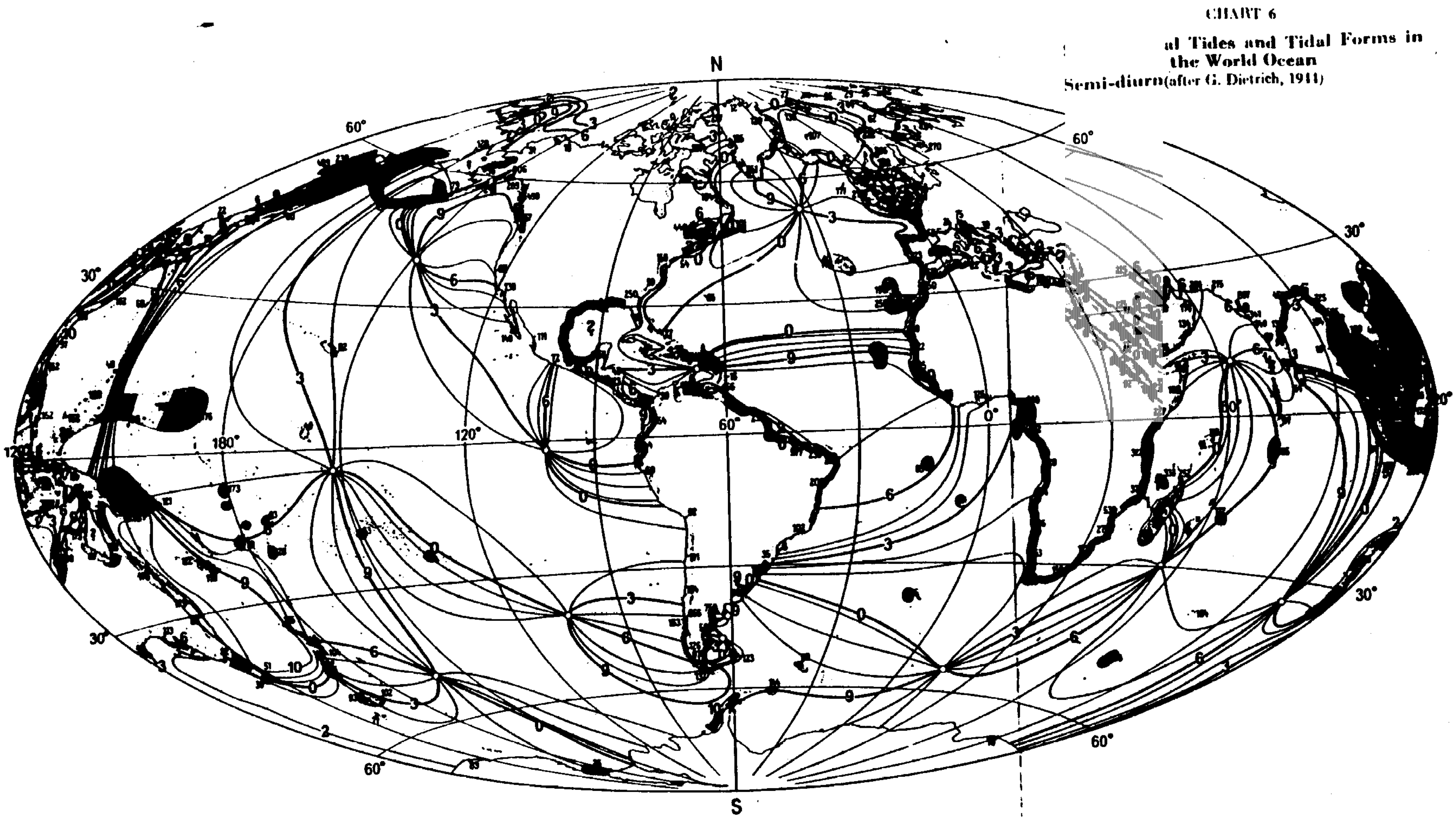

Figure 40(c). Positions of crests as a function of time for the M2 (Lunar Diurnal) tide. This is the largest tide. The next largest is the S2 (Solar Diurnal). Note that the time is is labeled in units of the period/12 and is not exactly hours, because the lunar day (time from moon overhead to moon overhead) is not 24 hours. Note that the wave circulates around single nodes (amphidromes) in the North and South Atlantic, but that there are four amphidromes in the Pacific south of the equator.

Figure 41 – Deep water capillary and gravity waves

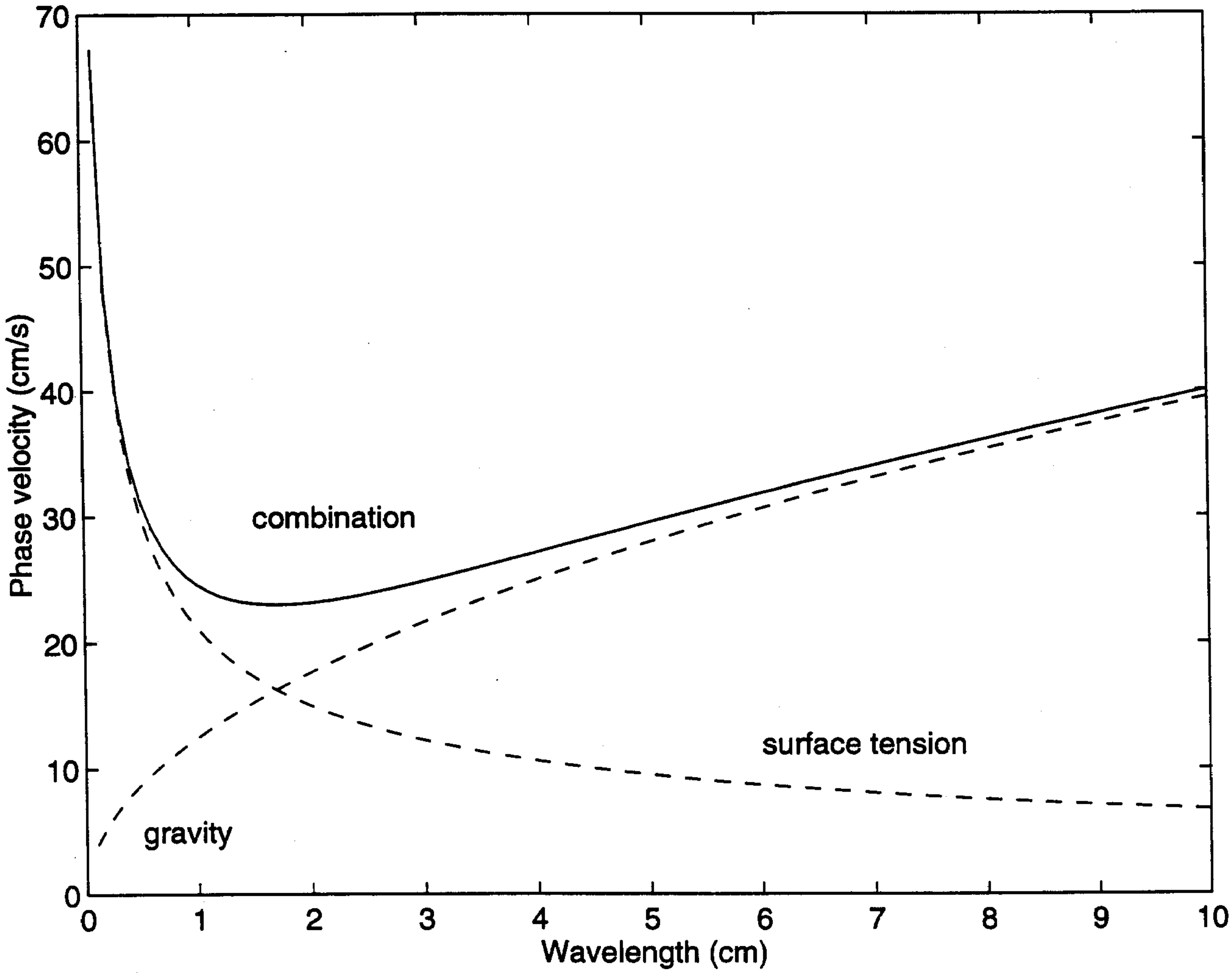

Figure 42

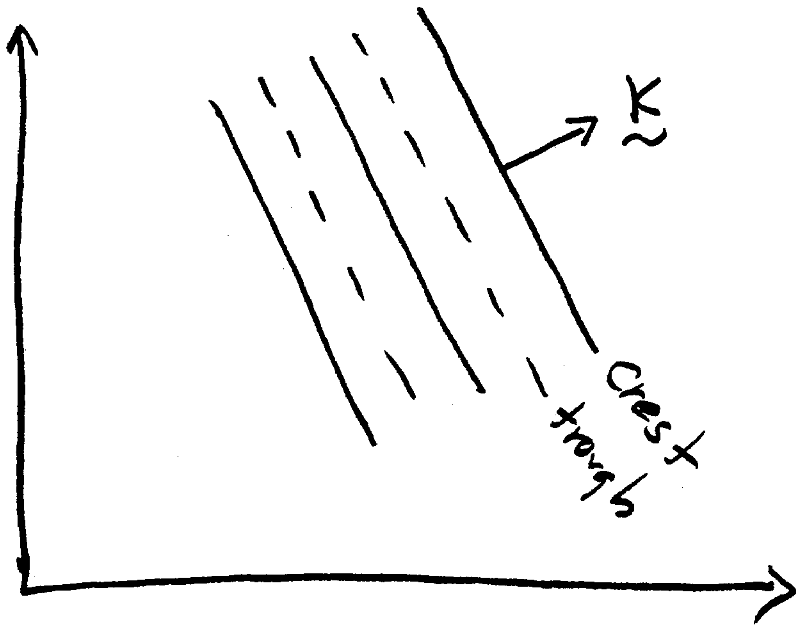

Phase $\phi = \underset{\sim}{k} \cdot \underset{\sim}{x} - \sigma t$

$\underset{\sim}{k} = k\hat{x} + l\hat{y} + m\hat{z}$

is $\perp$ to $\phi = \text{const}$ surfaces (ie $\perp$ to crest + troughs)

$\therefore$ To keep ϕ constant, observer must move $\perp$ to crest ($\parallel$ to $\underset{\sim}{k}$) at speed $\frac{\sigma}{|\underset{\sim}{k}|}$, which we call phase velocity.

FIGURE 43

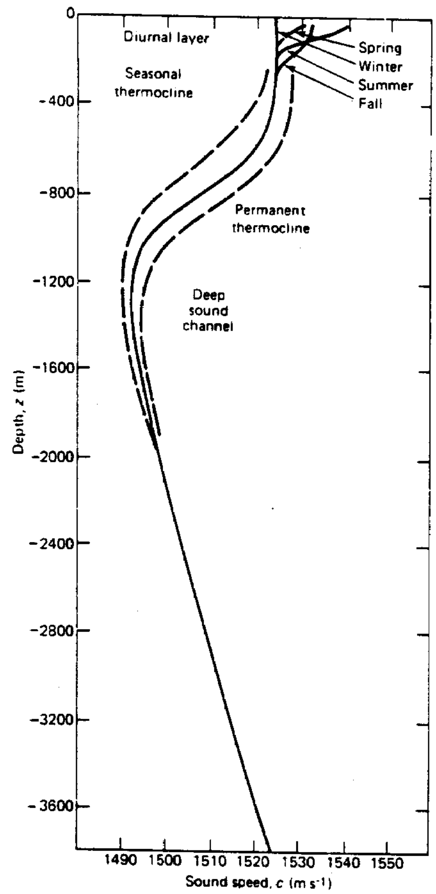

(a)

Sound speed profile from a station near Bermuda as averaged over nine years. [Adapted from Jones, L. M., and W. A. Von Winkle, *USN Underwater Sound Laboratory Report 632* (1965).]

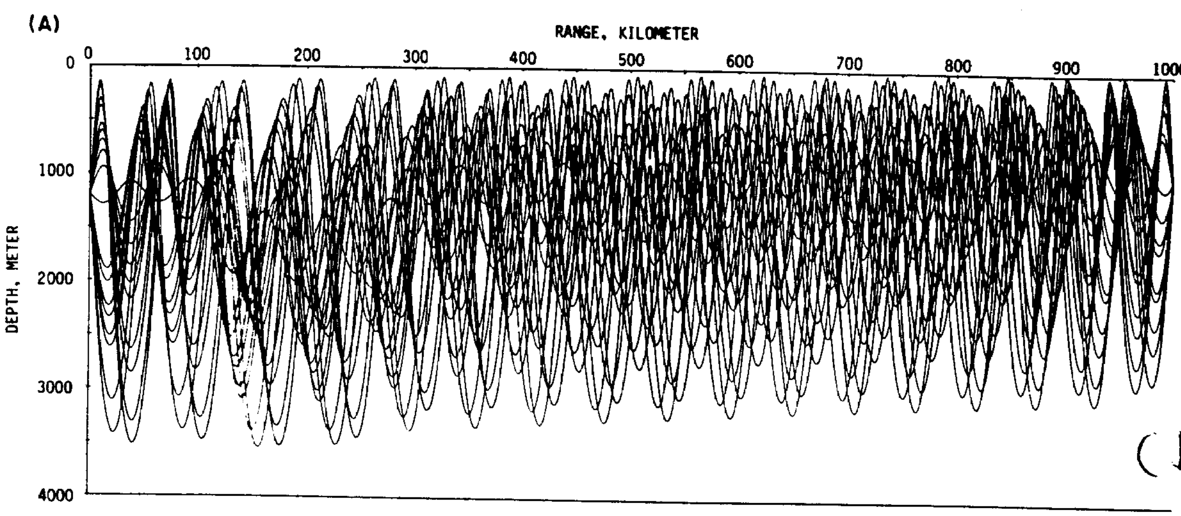

(b)

All the acoustic rays between a source (at 1200 m) and a receiver (at 1000 m) though a realistic ocean that includes a mesoscale warm eddy centered at 200 km downrange. From Mercer and Booker (1983).

FIGURE 43

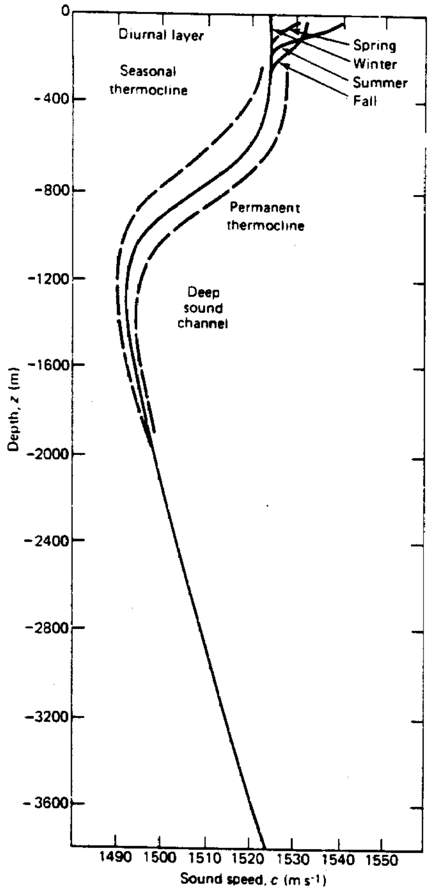

Sound speed profile from a station near Bermuda as averaged over nine years. [Adapted from Jones, L. M., and W. A. Von Winkle, *USN Underwater Sound Laboratory Report 632* (1965).]

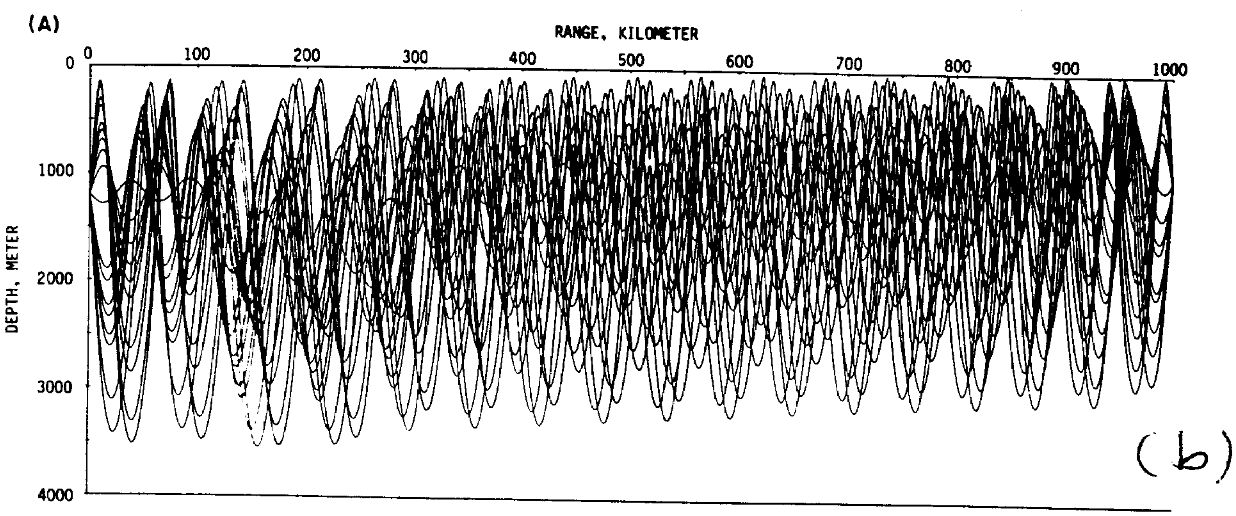

All the acoustic rays between a source (at 1200 m) and a receiver (at 1000 m) though a realistic ocean that includes a mesoscale warm eddy centered at 200 km downrange. From Mercer and Booker (1983).

Figure 47

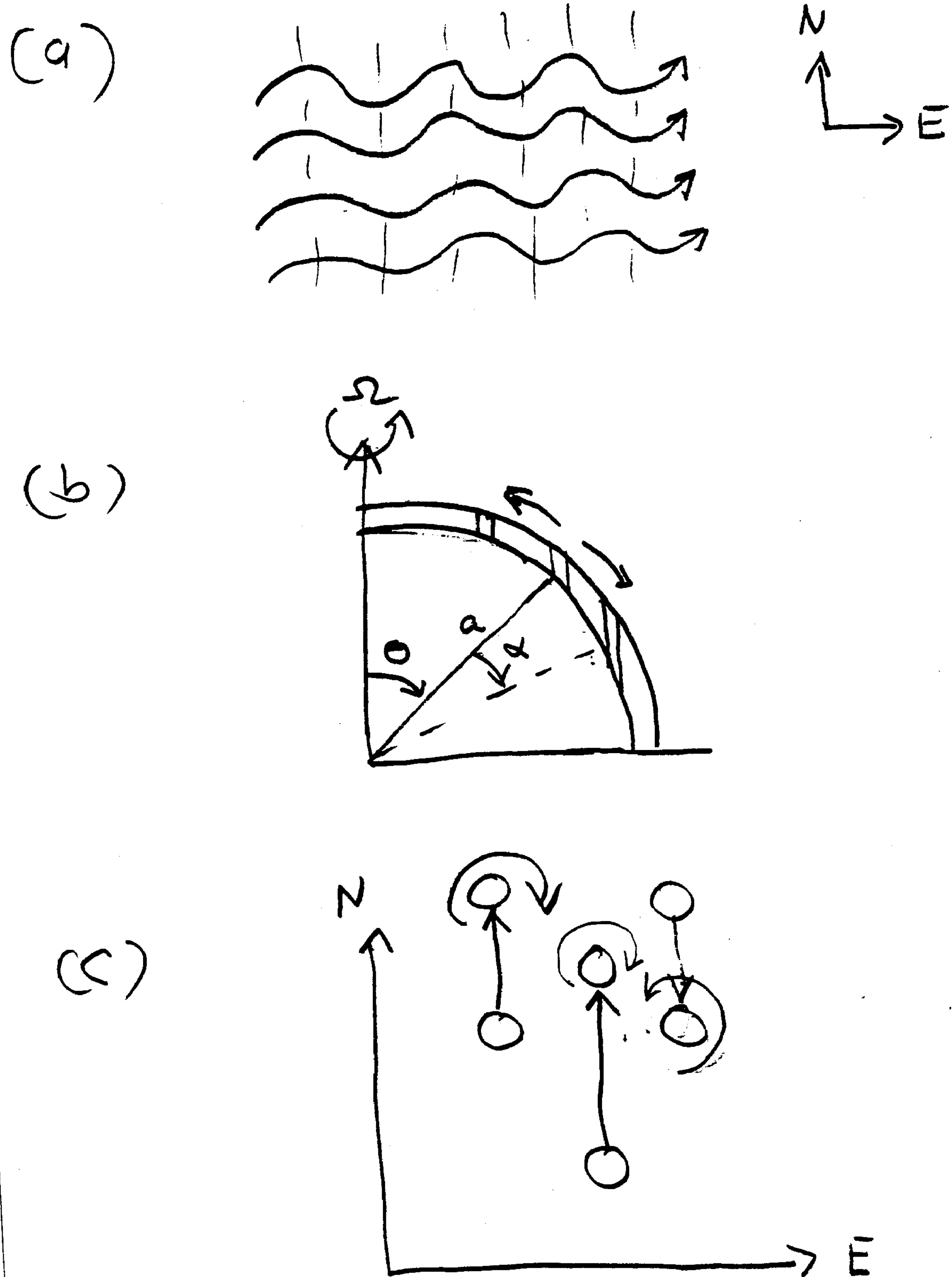

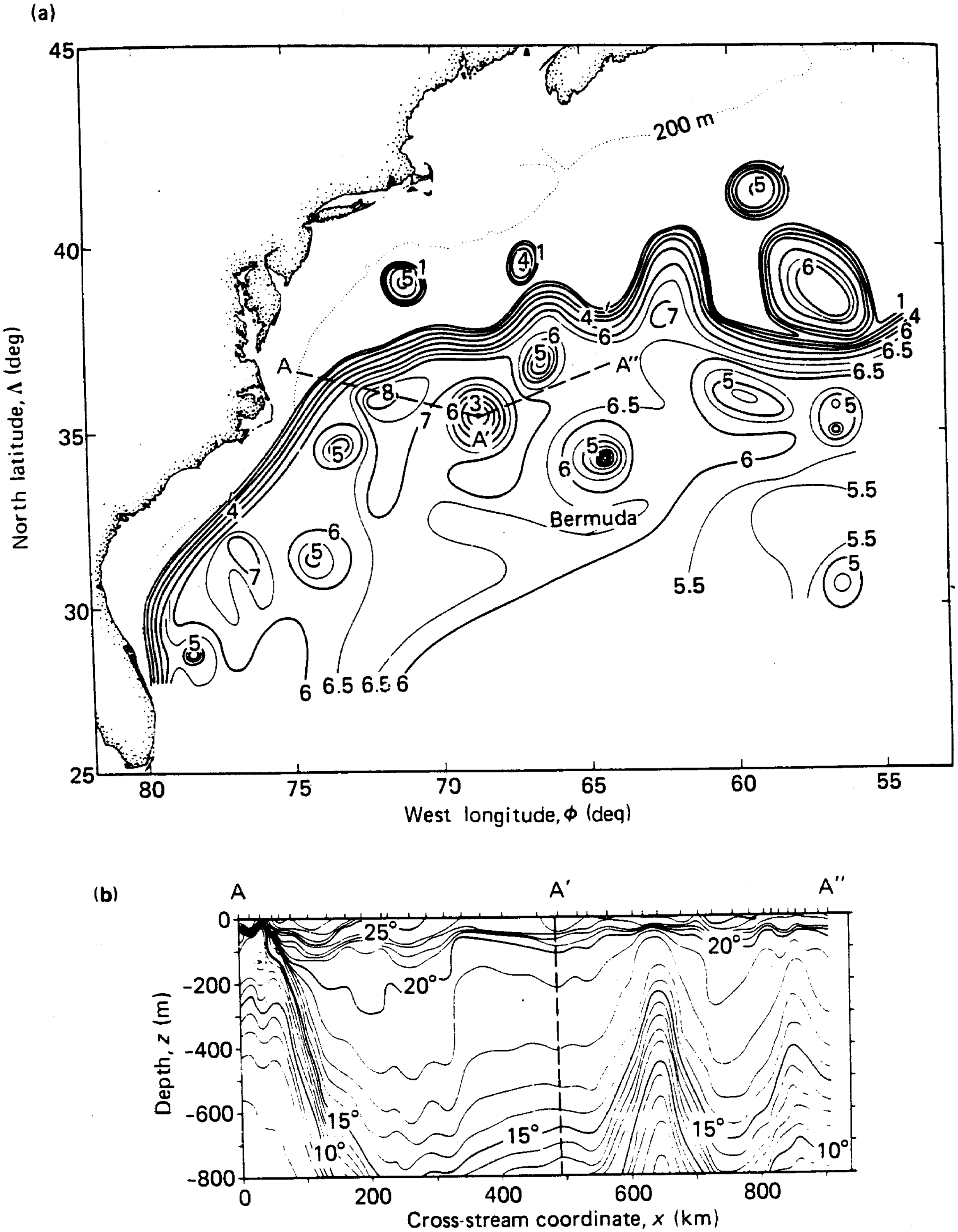

Fig. 4.5 (a) Positions of the 15°C isotherm at depths between 100 and 700 m, showing the Gulf Stream, nine cyclonic, and three anticyclonic eddies. Data were taken by subsurface drifting floats and other means. (b) Subsurface profile along a line segment A–A′–A″ in Fig. 6.42a, showing the Gulf Stream boundary at left, and cold-core rings at 650 and 850 km. [From Richardson, P., et al., *J. Geophys. Res.* (1978)].

FIGURE 46

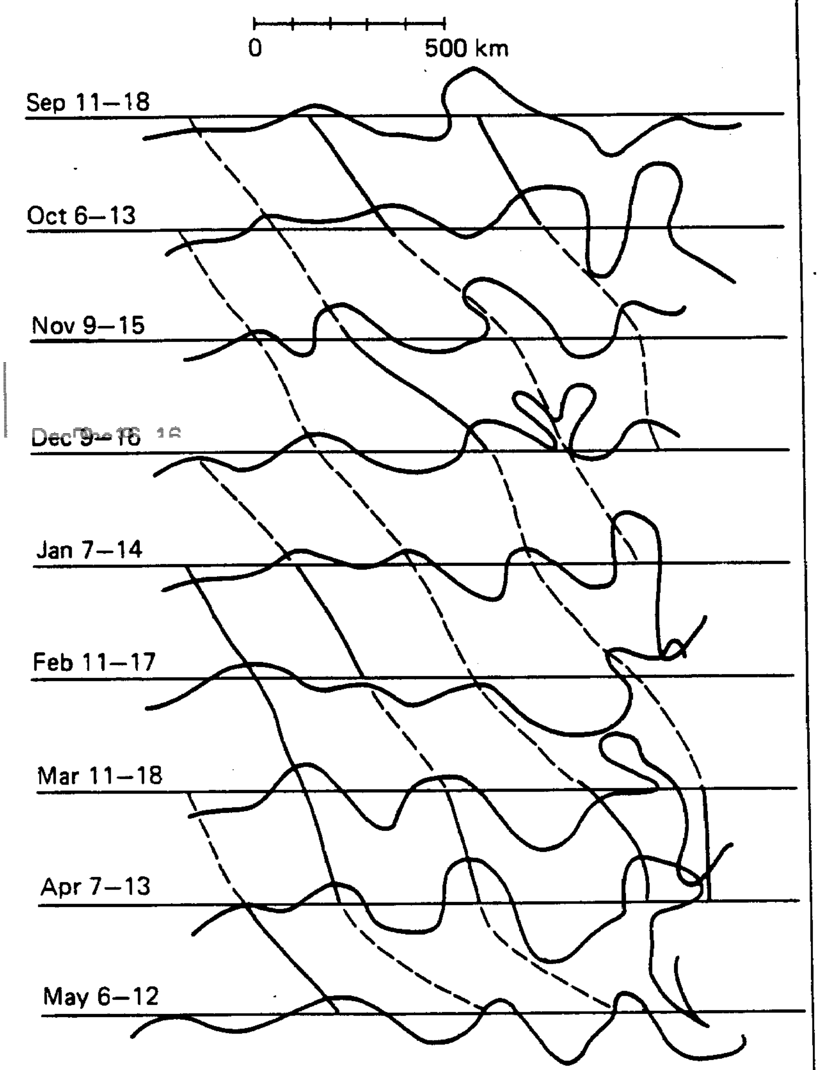

Phase progression, September 1965 – May 1966

FIGURE 47

(a)

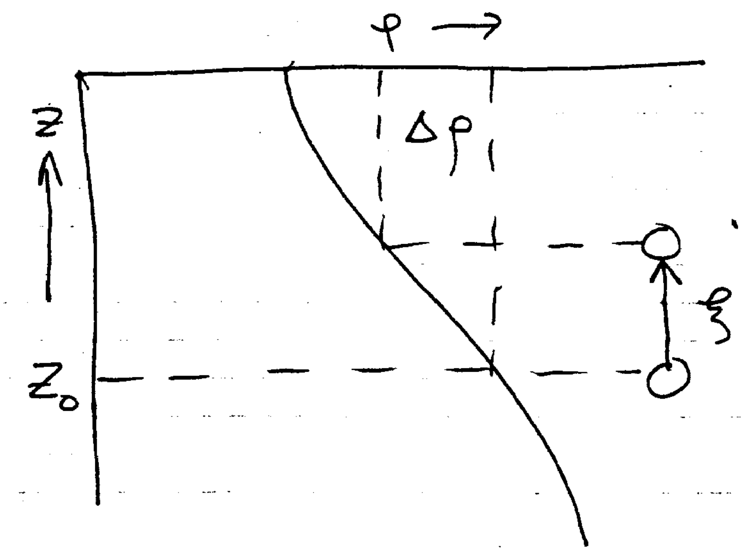

(b)

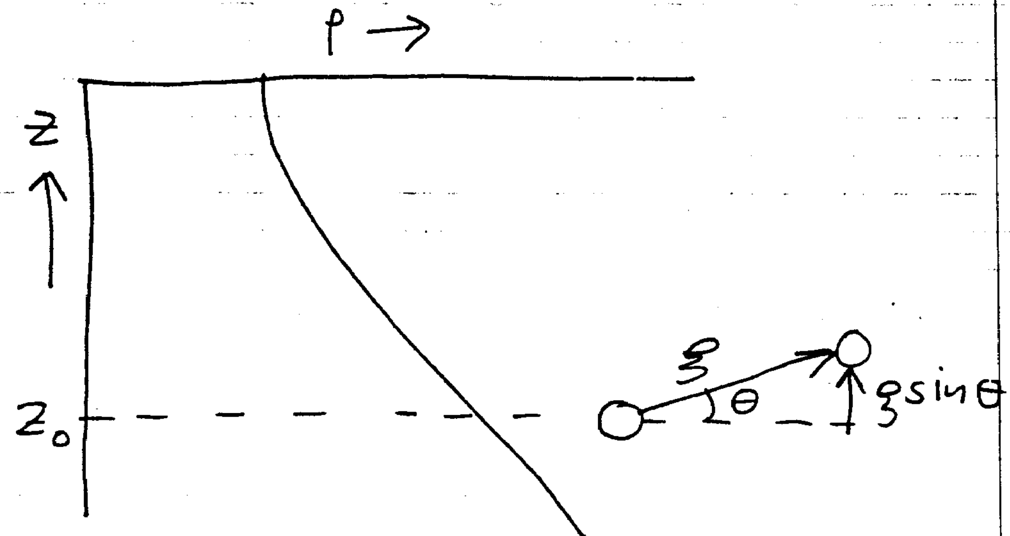

Restoring force in $\hat{z}$ direction $\propto \xi \sin\theta$

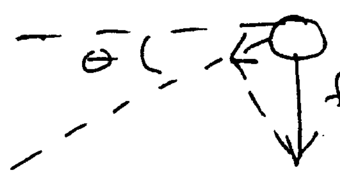

Restoring force directed towards original position $\propto \xi \sin^2\theta$

FIGURE 48

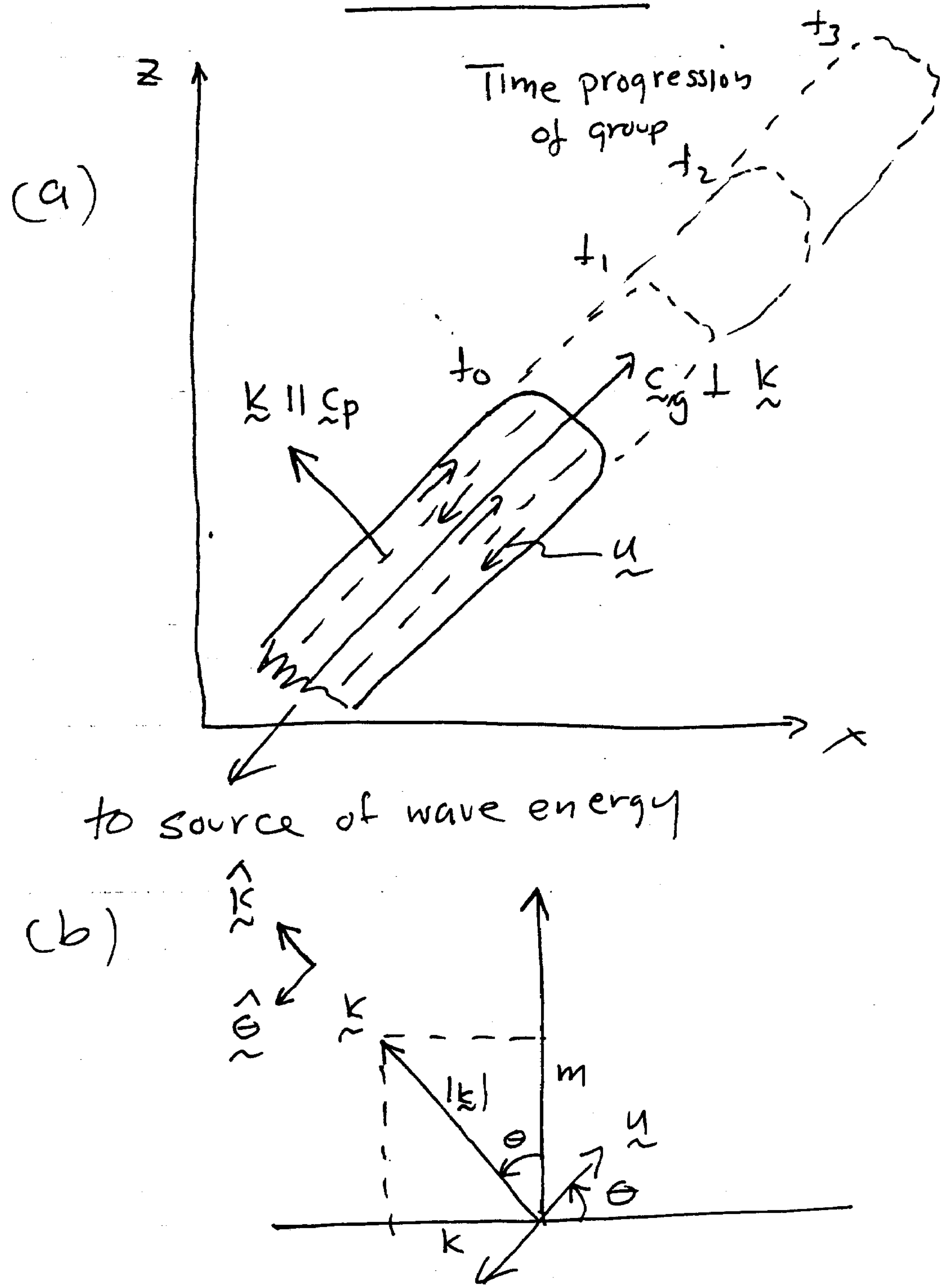

$$\sin\theta = \frac{k}{|\underset{\sim}{k}|} \; ; \; \cos\theta = \frac{m}{|\underset{\sim}{k}|}$$

FIGURE 49 (From Tritton)

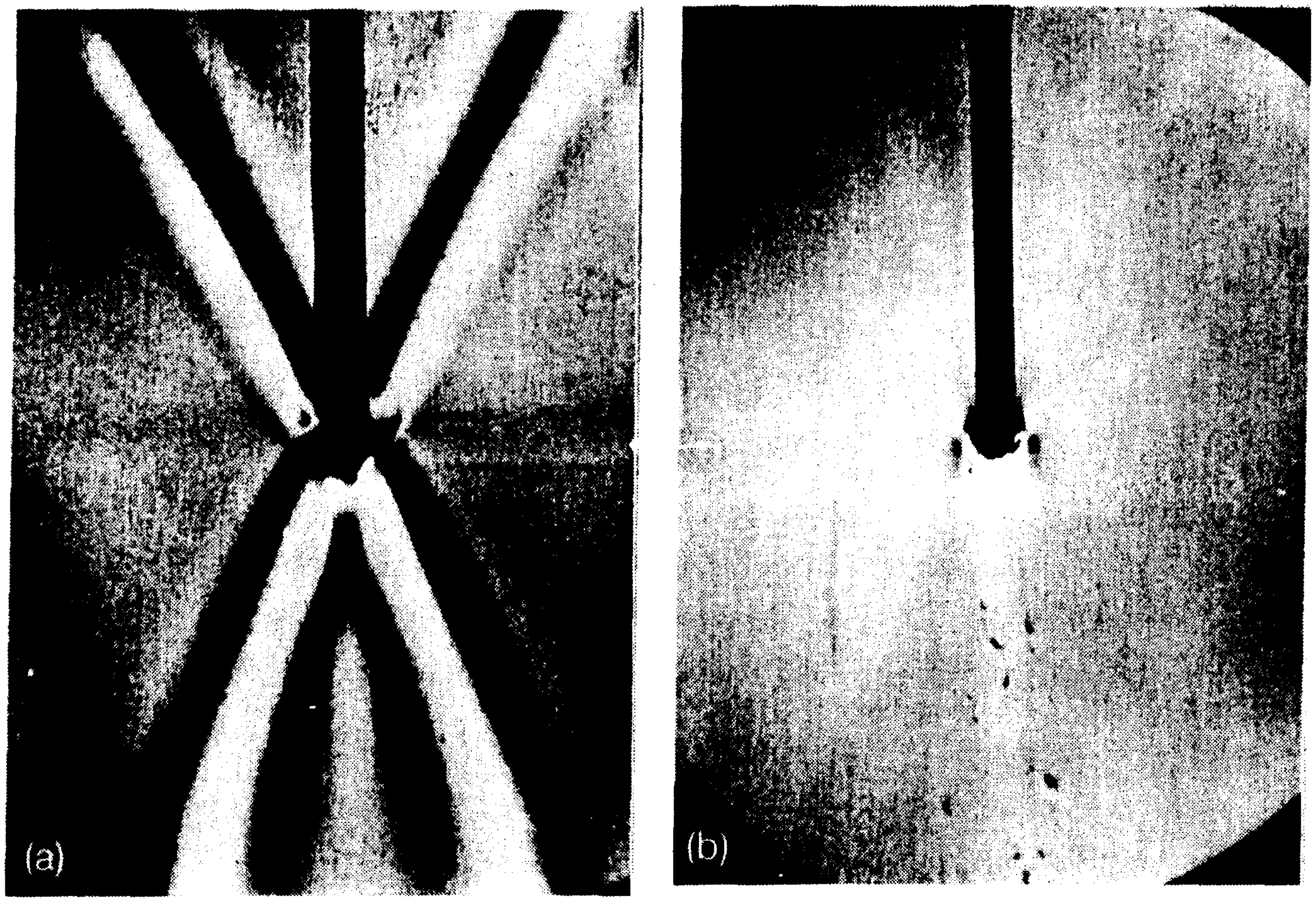

FIG. 15.11 Waves produced by vibrating cylinder in a stratified fluid (dark vertical line is cylinder support). (a) $\omega/N = 0.90$; (b) $\omega/N = 1.11$. Ref. [282].

FIGURE 50

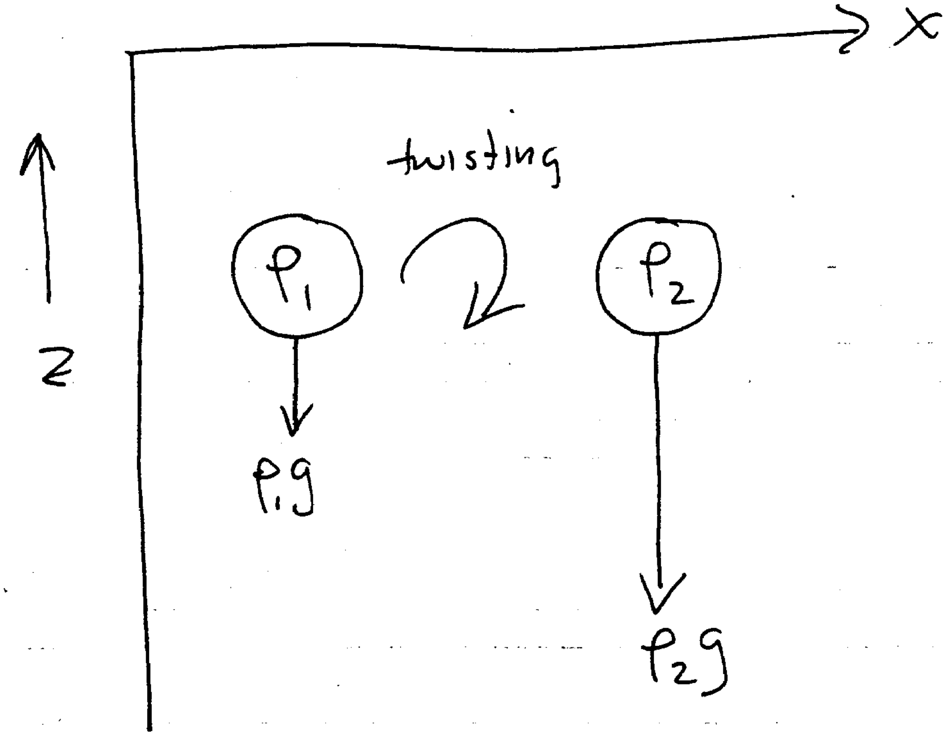

Generation of vorticity by lateral density variation

FIGURE 51

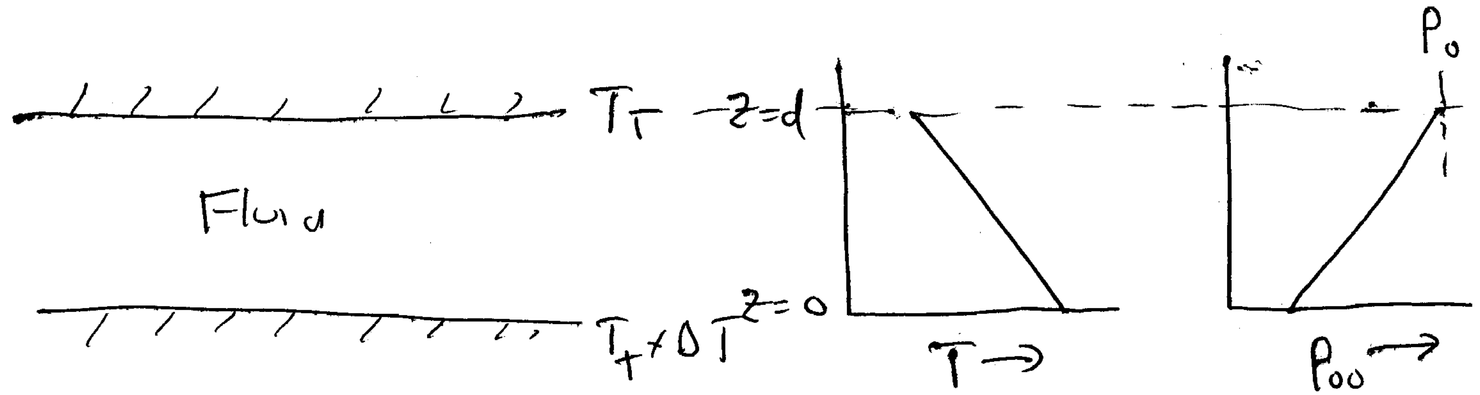

FIGURE 52

(a)

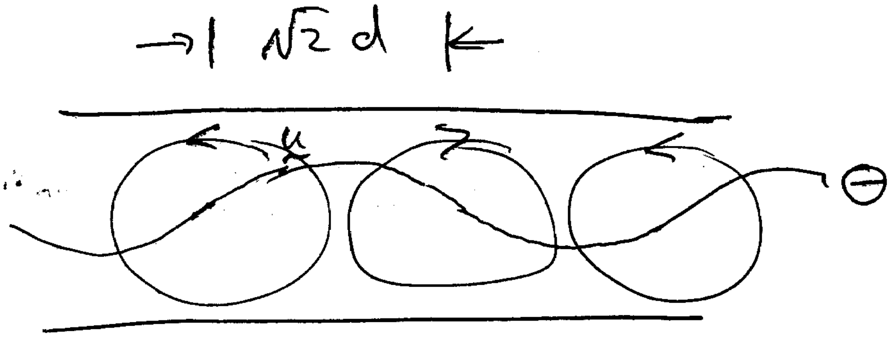

(b)

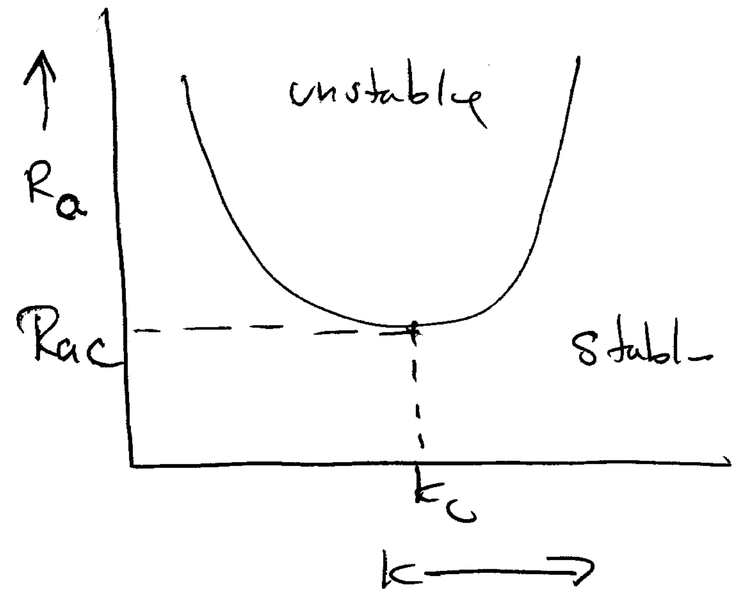

FIGURE 53

(a)

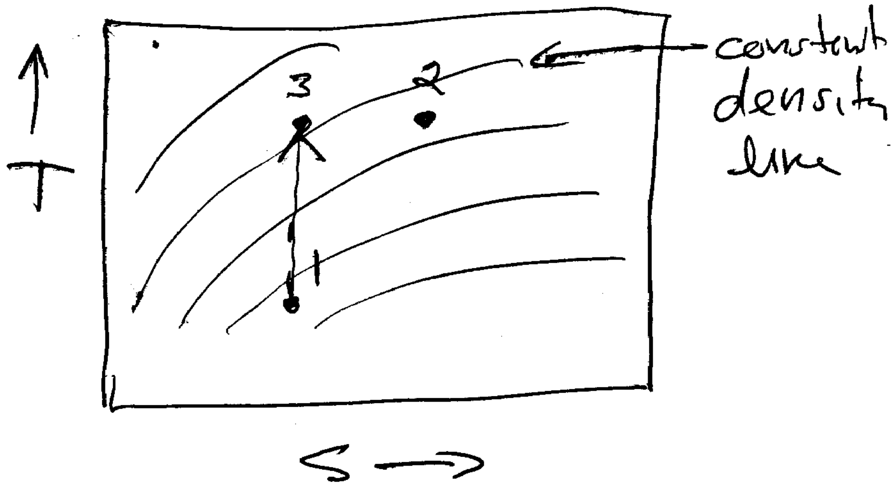

T
3
2
1
constant density line
S

(b)

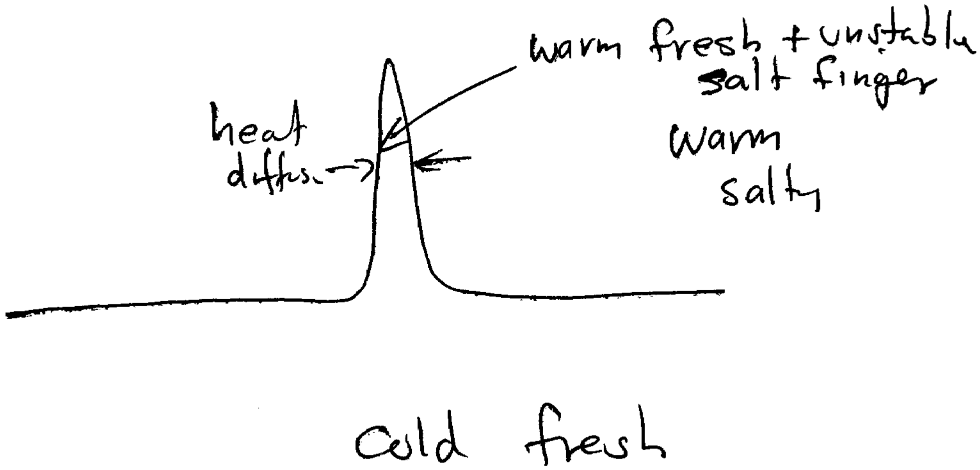

warm fresh + unstable salt finger
heat diffus.
warm salty
cold fresh